universität wien

MASTERARBEIT / MASTER'S THESIS

Titel der Masterarbeit / Title of the Master's Thesis

"From aneuploidy to drug resistance: insights into cellular adaptation"

verfasst von / submitted by

Lea Wallner, BSc

angestrebter akademischer Grad / in partial fulfilment of the requirements for the degree of

Master of Science (MSc)

Wien, 2023 / Vienna, 2023

Studienkennzahl lt. Studienblatt / degree programme code as it appears on the student record sheet:	UA 066 877
Studienrichtung lt. Studienblatt / degree programme as it appears on the student record sheet:	Genetik und Entwicklungsbiologie
Betreut von / Supervisor:	Assoz. Prof. Christopher Campbell, PhD

Acknowledgements

I would like to thank several people for their help during the work on this thesis. Firstly, I would like to thank Assoc. -Prof. Christopher Campbell, PhD, who provided me with the great opportunity to work on this research project. His guidance and expertise played an important role in expanding my understanding and development during my masters' research.

I am especially grateful to Tamara Klockner, who was not only an inspiring mentor, but also a great friend. Thank you for your invaluable support, input, encouragement, and kindness!

I would like to thank all my great lab mates for their helpfulness, support, and the great experience I have had.

Lastly, I want to express my deepest gratitude towards my family, friends and my partner for their unwavering support and encouragement.

Thank you!

Contents

Abstract

Aneuploidy, a state in which cells harbor an abnormal number of chromosomes, is common in cancer and usually detrimental to cell proliferation. Paradoxically, many tumors exhibit aneuploidy, which can enhance cell growth and therapeutic resistance. Chromosomal instability (CIN), arising from an increased rate of missegregation, can provide adaptive advantages in stressful environments. Drug induced CIN and the resulting cellular heterogeneity can lead to the acquisition of specific chromosome gains or losses, conferring resistance to the drug. In healthy cells, a surveillance mechanism called the spindle assembly checkpoint (SAC) ensures proper chromosome segregation. Its inhibition decreases mitotic timing and results in missegregation. Adaptation of dipHAP1 cells to the CIN-inducing SAC inhibitor reversine revealed that loss of chromosomes 6p or 13q rescued growth in reversine via elongation of mitotic timing. SAC genes *p31^{comet}* and *CDC16* on those chromosomes, respectively, were identified as key genes in this resistance (Adell & Klockner *et al*, 2023). Throughout this thesis, I tested the overexpression of *p31^{comet}* and *CDC16* via CRISPRa in dipHAP1 cell lines heterozygous for those genes. The elongation of mitotic timing upon overexpression with and without reversine further strengthened the role of those genes in reversine resistance. Through selection of reversine adapted cell lines with gains of specific chromosomes we wanted to test their roles in reversine resistance. CRISPR deletions of gained chromosome arms revealed gain of chr arm 1, the acquisition of which does not only reduce mitotic timing, but also errors, to be involved in reversine resistance.

Keywords: Aneuploidy, drug resistance, chromosome gains/losses

1 Introduction

1.1 Chromosome segregation

The accurate division of replicated chromosomes during mitosis into daughter cells is essential for the continued proliferation of cells. If mitosis is successful, each daughter cell ends up with exactly half the mother's genetic information. In eukaryotes, the separation of chromosomes during anaphase is driven by forces exerted by a spindle mainly consisting of microtubules associated with motor proteins. During metaphase, microtubules attach to the chromosomes at the kinetochore, a complex proteinaceous structure that assembles at the centromeres of both chromatids. Each of the sister chromatids has to attach at the kinetochore to microtubules emerging from opposite spindle poles in a state termed bi-orientation (Tanaka, 2005; Anjur-Dietrich *et al*, 2021). To make sure that all chromatids are attached to spindle microtubules, a surveillance mechanism called the spindle assembly checkpoint (SAC) is employed. When chromosomes are not attached to spindle microtubules, the SAC delays progression into anaphase until all kinetochore-microtubule connections are established. (Holland & Cleveland, 2012; Lara-Gonzalez *et al*, 2021). If any microtubules are connected incorrectly, intervention by proteins of the chromosomal passenger complex (CPC) leads to the detachment of the incorrect connections This activates the SAC for a new attempt at establishing the microtubule-kinetochore connections (Krenn & Musacchio, 2015).

1.2 Aneuploidy and its consequences

In the case that cells have errors in chromosome segregation, chromosomes are unequally divided between the two daughter cells. This resulting state defined by an abnormal number of either whole chromosomes or chromosome arms is called aneuploidy (Ben-David & Amon, 2020; Sansregret *et al*, 2018). Each passing second, millions of cells divide (Anjur-Dietrich *et al*, 2021) with chromosome missegregation rates below 1% in healthy diploid tissue. An increased rate of chromosome missegregation is called chromosomal instability (CIN). Cancer cells, that are chromosomally unstable, exhibit much higher missegregation rates (Maiato & Silva, 2023; Nicholson & Cimini, 2013).

While being extremely common, aneuploidy is usually detrimental for proliferation and in humans a major cause of miscarriages and intellectual disabilities. Only a few aneuploidies like trisomy 21 are viable (Hassold & Hunt, 2001).

As chromosomes can carry thousands of genes, gain or loss of even a single chromosome leads to massive changes in gene dosages. While dosage compensation can occur, expression levels of genes on aneuploid chromosomes often scale proportionally and can even influence gene expression on other chromosomes (Kojima & Cimini, 2019; Kahlem *et al*, 2004; Schukken & Sheltzer, 2022). The presence of just one additional chromosome can have detrimental effects like changes in cellular metabolism or delay in proliferation (Williams *et al*, 2008; Torres *et al*, 2007; Thorburn *et al*, 2013). In yeast, aneuploidy can sensitize cells to DNA damage, impair DNA repair and induce genomic instability (Sheltzer *et al*, 2011). Furthermore, aneuploidy can lead to the accumulation of misfolded proteins increasing proteotoxic stress from intracellular protein imbalances, further promoting genomic instability (Torres *et al*, 2007; Sheltzer *et al*, 2011). Just like the studies conducted in yeast cells, in human cells aneuploidy can lead to a variety of issues, including replication stress, DNA damage and genomic instability (Passerini *et al*, 2016; Santaguida *et al*, 2017).

With the knowledge that aneuploidy can impact cell growth negatively, it seems counterintuitive that approximately 90% of solid tumors and ~75% of hematopoietic cancers display aneuploidy (Ben-David & Amon, 2020; Weaver & Cleveland, 2008). Aneuploid cancers are implicated in worse prognosis, resistance to chemotherapeutics and tumor progression (Lee *et al*, 2011; Lukow *et al*, 2021; Weaver *et al*, 2007). This discrepancy is termed the “aneuploidy paradox” (Weaver & Cleveland, 2008).

1.3 Mechanisms of aneuploidy and CIN acquisition

While it is commonly stated that CIN leads to the acquisition of aneuploidies, aneuploidy itself can induce CIN. Even the gain of a single chromosome can lead to DNA damage and genomic instability through compromised DNA replication (Passerini *et al*, 2016; Tijhuis *et al*, 2019). The more common path, however, is CIN resulting in chromosome gains or losses. The Bi-orientation of chromosomes is ensured by the spindle assembly checkpoint (SAC) and its effector, the mitotic checkpoint complex (MCC). It sends a signal

to stop anaphase if it detects unattached kinetochores and prevents premature segregation of chromosomes. Kinetochores that are not attached to the mitotic spindle are bound by SAC components and cell cycle progression is stopped until new connections to microtubules are established (Musacchio, 2015). Defects in SAC components lead to early onset of anaphase, resulting in missegregation and aneuploidy. While SAC defects can predispose to cancer, most tumors have no impairment in SAC signaling. However, aneuploidy can sensitize cells to inhibition of the SAC, making it a potential target for cancer therapies (McAinsh & Kops, 2023; Thompson *et al*, 2010).

The kinetochore-microtube attachment is reversible, which is necessary for the correction of possible erroneous attachments. Sometimes kinetochores become attached to both spindle poles, which is termed merotely, or both kinetochores of a chromosome tether to the same pole, termed syntelic attachment. The destabilization of such erroneous attachments is regulated by the Aurora B kinase, which is part of the chromosomal passenger complex (CPC). Overly stabilized attachments due to imbalances in associated proteins, like members of the Ndc80 complex, hinder the correction of syntelic or merotelic attachments. This results in an increased amount of lagging chromosomes and missegregation (Krenn & Musacchio, 2015; DeLuca *et al*, 2006; Thompson *et al*, 2010). Cohesion defects like early loss of cohesion between sister chromatids can result in mitosis defects and missegregation of chromosomes (Nasmyth & Haering, 2009). Additionally, centrosomes, which organize the microtubules at the spindle poles, can amplify, leading to supernumerary centrosomes and the formation of multipolar spindles. This results in massive missegregation and likely death of the daughter cells. Supernumerary centrosomes can cluster together to form two poles, however, enrich for merotelic attachments, lagging chromosome and missegregation, but can produce viable progeny (Holland & Cleveland, 2012; Ganem *et al*, 2009). The arise of aneuploidy is accompanied by activated p53 signaling in MEFs and p53 knockout (KO) can accelerate the development of tumors in mice (Li *et al*, 2010).

1.4 Spindle assembly checkpoint (SAC)

As mentioned previously, the SAC is a surveillance mechanism that monitors correct kinetochore-microtubule attachments during mitosis and therefore ensures the proper segregation of chromosomes (Figure 1). The basic principle of the SAC is, that it ensures cell division halts until every chromosome is correctly and stably attached to microtubules arising from the polar spindle poles in a bi-orientated manner. The microtubules attach to the kinetochores that assembles at the centromeres of chromatids. While the inner kinetochore is bound to centromeric nucleosomes, the outer kinetochore connects to microtubules. In humans, one kinetochore binds about 10 microtubules and the number of bound microtubules is implicated in regulation of SAC signaling strength (McAinsh & Kops, 2023; Cheeseman, 2014).

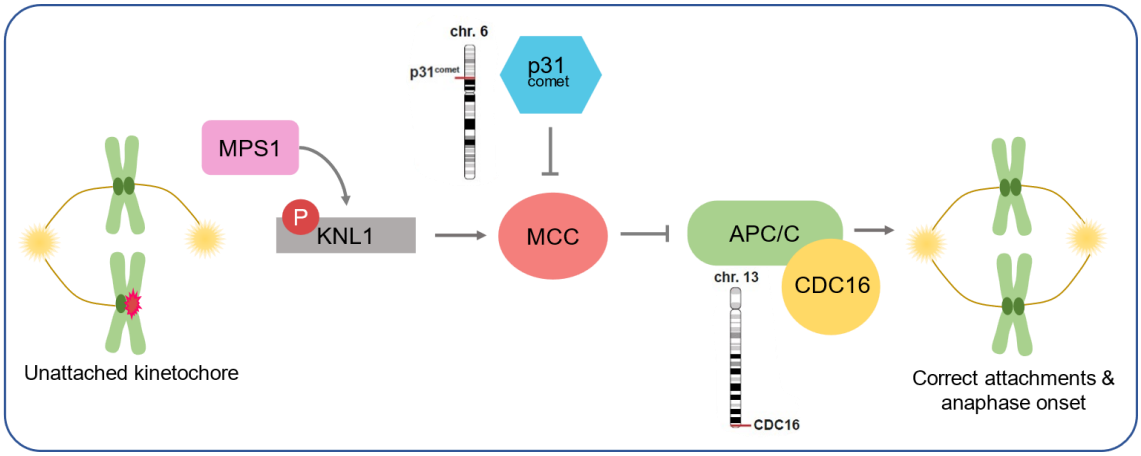

Figure 1: Simplified model of the spindle assembly checkpoint (SAC). Unattached kinetochores are sensed by SAC signaling molecules. Upon phosphorylation of kinetochore proteins by MPS1, the mitotic checkpoint complex (MCC) is activated and inhibits the APC/C (anaphase promoting complex) until the attachment is fixed. APC/C is then activated, and the cell cycle progresses into anaphase. $P31^{comet}$ is an inhibitor of the mitotic checkpoint complex and CDC16 part of the APC/C.

Active SAC signaling inhibits the function of the E3 ubiquitin ligase APC/C (anaphase promoting complex/ cyclosome). One of the APC/C components is called CDC16. In its active form, APC/C leads to the destruction of anaphase inhibitors cyclin B1 and securin, promoting anaphase. At unattached kinetochores, the kinase MPS1 phosphorylates the outer kinetochore protein KNL1, which triggers the production of the mitotic checkpoint complex (MCC). The tetrameric MCC, consisting of MAD2, BUB3, BUBR1 and CDC20, can bind the APC/C, inhibiting its function. Once a stable end-on connection between all kinetochores and microtubules is achieved, the production of MCC is stopped and the

SAC is silenced. This SAC-silencing is dependent on the activity of phosphatases PP1 and PP2A-B56, while MCC disassembly is promoted by the activity of proteins TRIP13 and p31^{comet}. The silencing is followed by liberation of the APC/C, which cleaves its targets and anaphase is started (McAinsh & Kops, 2023; Lara-Gonzalez *et al*, 2021; Sansregret *et al*, 2017).

To ensure segregation fidelity, cells need to be able to sense not only unattached, but also incorrectly attached microtubules. Correction of attachment errors is accomplished by the kinase Aurora B, which is part of the CPC. Aurora B can reduce the kinetochore-microtubule affinity by phosphorylation of the outer kinetochore protein NDC80, resulting in destabilization of the connection and freeing of the kinetochore (McAinsh & Kops, 2023; Carmena *et al*, 2012).

1.5 Aneuploidy and CIN as adaptive advantage

While aneuploidy and chromosomal instability are often associated and aneuploidies can arise through CIN, they are distinct from each other. While CIN describes the accelerated acquisition of aneuploidies through continued missegregation, aneuploidy solely describes the karyotype (Vasudevan *et al*, 2021). Also, while aneuploidy and CIN often appear in simultaneously, not all aneuploid tumors are necessarily unstable (Ben-David & Amon, 2020). An intrinsic property of chromosomal instability, but not aneuploidy in general, is that it can confer multidrug resistance (Lee *et al*, 2011). CIN and the continued missegregation that comes with it, lead to the generation of a heterogeneous cell population, in which some cells can have proliferative advantages through the random acquisition of beneficial aneuploidies that outgrow less fit clones. Inducing CIN through treatment with anti-cancer drugs can accelerate the rate at which cells adapt and ultimately display resistance. Upon CIN induction, beneficial aneuploidies are positively selected for, like chromosome 11 trisomy or loss of chromosome 10 in taxol-resistent RPE1 cells (Lukow *et al*, 2021; Ippolito *et al*, 2021). After prolonged CIN induction, *CDC16* and *p31^{comet}*, genes involved in SAC signaling, and losses of their respective chromosome have been associated with increased resistance to the drug reversine (Adell & Klockner *et al*, 2023). Even transient CIN-induction can lead to malignant transformation in *p53*-KO mice (Shoshani *et al*, 2021). However, CIN does not immediately confer a fitness advantage. On the contrary, very high rates of missegregation are detrimental for

proliferation and lead to cell death. Therefore, the induction of overwhelming CIN has been suggested as a cancer treatment (Lukow *et al*, 2021; Silk *et al*, 2013).

When cells are exposed to high rates of chromosome missegregation through induction of CIN, for example through SAC inactivation, acquisition of initial aneuploidies can help the cells in survival at least temporarily. Further tweaking of aneuploid chromosomes provides cells with selective advantages and gradually increases their growth. Despite the differences in initial aneuploidies, cells converge upon an ideal complex karyotype, both in yeast as well as in human cells. Genes on the aneuploid chromosomes can help alleviate the burden that aneuploidy and CIN impose on cells (Ravichandran *et al*, 2018; Adell & Klockner *et al*, 2023). After cells adapted through their karyotype, specific point mutations can emerge that further decrease CIN and aneuploidy (Clarke *et al*, 2023).

1.6 Aneuploidy patterns

Aneuploidy relies on genomic context, not every gain or loss has the same advantage for every type of cancer. Some aneuploidies are found in a great variety of cancer types like gain of chromosome 20 or loss of chromosome 13 (Knouse *et al*, 2017). Certain tumors exhibit patterns of aneuploidy, that are not as frequently observed in cancer overall, like in gastrointestinal tumors gain of 13q, or the loss of chr. 10 in glioblastomas (Vasudevan *et al*, 2021; Taylor *et al*, 2018). These complex, cancer specific patterns present challenges in discerning the underlying selective advantages of such aneuploidies. In human cells, long term adaption to the MPS1 inhibitor reversine led to the emergence of aneuploidy patterns, that on the one hand were cell-type specific, but on the other hand recapitulated patterns found across all types of cancers like gains of chromosome 1q or 8. This points to the conclusion, that certain aneuploidies confer general fitness advantages, regardless of the microenvironment (Adell & Klockner *et al*, 2023). A single gain of chromosome 5 can increase invasiveness and induce partial epithelial-mesenchymal transition in colon cancer cells in vitro (Vasudevan *et al*, 2020).

The balance of tumor-driver and -suppressor genes across chromosomes has been implicated in predicting the frequency of gain and loss of chromosomes (Davoli *et al*, 2013). Such genes, like *RAD21* and *MYC* are likely connected to selection of chr. 8 trisomy in Ewing sarcomas (Su *et al*, 2021). Gain of p53-suppressor gene *MDM4* via the

acquisition of 1q trisomy promotes growth in cancer and is required for further proliferation of cells harboring this aneuploidy, but only in cells without *TP53* mutations. Such a mechanism, in which a cell requires an aneuploidy for proliferation, is termed “aneuploidy addiction” and a potential therapeutic target (Girish *et al*, 2023).

Identifying cancer-specific patterns holds treatment potential as certain aneuploidies harbor unique vulnerabilities, like increased sensitivity of cells loosing chr. 8p against autophagy inhibitors (Ben-David & Amon, 2020; Cai *et al*, 2016). Both haploinsufficiency as well as triplosensitivity could be potential therapeutic targets (Ben-David & Amon, 2020). A lot of cancers harbor an array of different aneuploidies, making it difficult to target single chromosome alterations (Vasudevan *et al*, 2021), but the development of such complex karyotypes does not just benefit cancers. These cells show increased levels of cell-surface proteins, that mediate the activation of natural killer (NK) cells and their removal in vitro. This might be a potential pathway through which the immune system can recognize aneuploid cancer cells, before they can evade immune surveillance (Santaguida *et al*, 2017).

1.7 Aim of this study

Digging deep into the details of specific aneuploidies, chromosome gains and losses plays a big role in genetic research. It helps deepen our understanding of the complex world of cancer biology and figure out drug resistance mechanisms. As previously established, certain aneuploidies can provide growth advantages in specific circumstances (Lukow *et al*, 2021; Ippolito *et al*, 2021). Along similar lines, we wanted to explore the role of aneuploidies in drug resistance. In their 2023 paper, Adell & Klockner et al. (Adell & Klockner *et al*, 2023) adapted multiple populations of different cell lines to long-term SAC inactivation via the drug reversine, a MPS1 inhibitor. The high rates of CIN that were induced by the treatment led to cells adapting to the drug via selective accumulation of aneuploidies. They found that individually adapted populations of the same cell line converged upon very similar karyotypes over the 90 days of adaptation, establishing aneuploidy patterns. Aneuploidy patterns were either shared among multiple cell lines or were cell type-specific. In multiple cell lines including dipHAP1, derived from chronic myeloid leukemia, among other changes, loss of chromosome 13q was frequently observed over the 90-day adaptation period, whereas in immortalized retina epithelial

cells (RPE1) specifically, loss of chromosome 6p was common (Figure 2A). The identification of correlations between cell populations exhibiting these aneuploidies and their improved resistance to reversine, compared to populations without these specific aneuploidy patterns, emphasizes their role in the adaptation to reversine.

Using this information, they engineered dipHAP1 cells, using the CRISPR/Cas9 system, with chromosome 6p or 13q monosomies, respectively. Those chromosome losses led to better growth in reversine measured by colony formation assays. Additionally, those monosomies increased mitotic timing (Figure 2B) and were able to reduce missegregation of chromosomes (Figure 2C). They were then able to identify genes on those chromosome arms that, if homo- or heterozygously deleted, were sufficient to increase reversine resistance, extend mitotic timing and increase alignment. On chromosome 6p, that gene is *p31^{comet}*, which promotes the disassembly of the MCC. On chromosome 13q it is *CDC16*, a component of the APC/C (Figure 2B). Previously, inhibition of *CDC16* has been shown to increase mitotic duration and reduce mitotic errors in reversine treated cells (Sansregret *et al*, 2017).

Apart from chromosome losses, prevalent changes in karyotype upon adaptation included gains of chromosome 1, 5, 8 and 20. Those chromosome gains can also be found in several cancers (Knouse *et al*, 2017). This could point to those aneuploidies conferring a general growth advantage, as opposed to being reversine specific.

In my master thesis, I firstly aimed to determine further whether the copy number losses of *p31^{comet}* and *CDC16* are the only drivers of the observed aneuploidy patterns of 6p loss and 13q loss. To investigate this, I implemented the CRISPRa system to overexpress *p31^{comet}* and *CDC16* in the 6p and 13q monosomic dipHAP1 cell lines. I used live cell microscopy to determine changes in mitotic timing upon overexpression of the target genes in comparison to the monosomic cell lines.

Secondly, I aimed to identify whether chromosome gains acquired during the reversine adaptation were similarly involved in reversine resistance or if their gain led to a broader fitness advantage. To determine the role of frequent chromosome gains, I employed the CRISPR/Cas9 system to revert acquired chromosome gains back to a euploid state by deleting one chromosome copy in reversine adapted dipHAP1 and HAP1 cell lines. To discern any potential benefits conferred by the acquired chromosome gains compared to

the deletion cell lines, I measured mitotic timing using live cell microscopy, as well as conducting wound healing and colony formation assays.

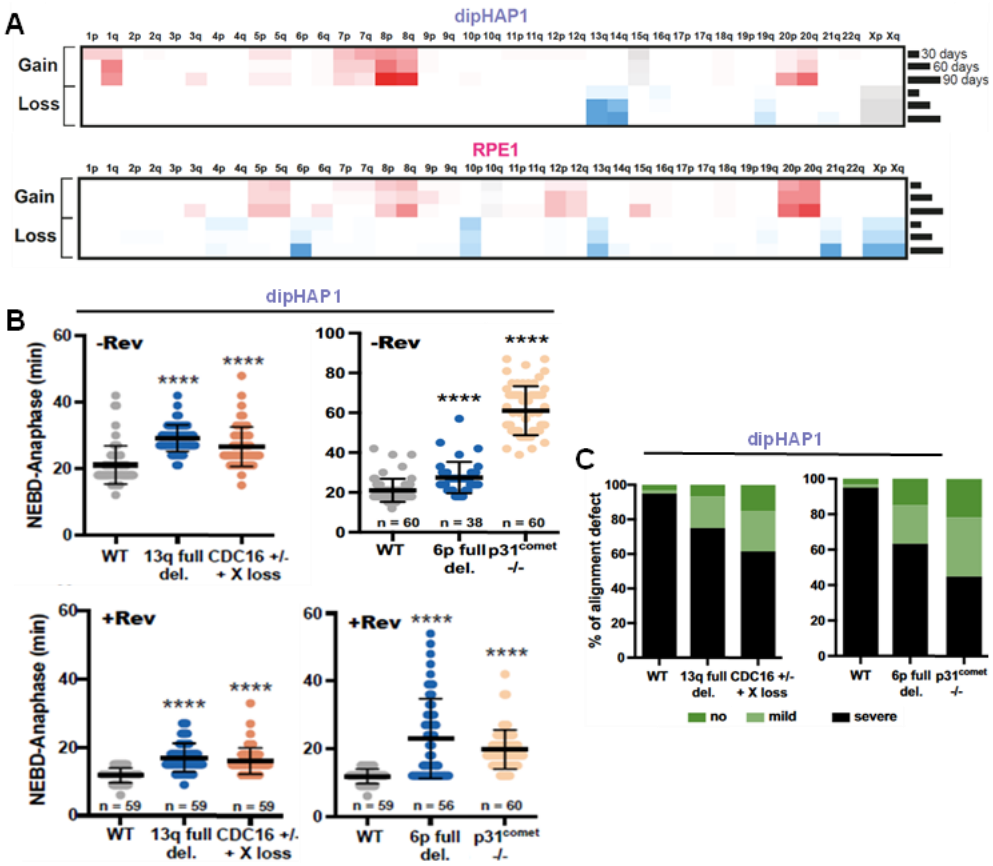

Figure 2: Cell lines adapted to reversine show increased mitotic timing and decreased mitotic errors. Figure adapted from Adell & Klockner et al., 2023 (Adell & Klockner et al, 2023). (A) Pattern of gains and losses seen during reversine adaptation process. (B) Measurement of mitotic duration as time from NEBD-anaphase in minutes without (-Rev) or with (+Rev) reversine. (C) Quantification of no, mild (1 unaligned chromosome) and severe (multiple unaligned chromosomes) alignment defects.

2 Methods

2.1 Cell lines and cell culture

For the experiments in this thesis, HAP1 (p53-/-) and dipHAP1 (p53-/-) cells were used (Table 9). All cell lines were cultured at 37°C with 5% CO_2 in a humidified incubator using IMDM (Sigma-Aldrich) media with 10% FBS and 1% Penicillin-Streptomycin. Cells were split using trypsin-EDTA (Sigma Aldrich) for dissociation about every 2-3 days depending on confluency and experiment. Generally, HAP1 cells were kept at slightly lower confluency than dipHAP1 cells. Cell lines that were used in experiments were usually not cultured for longer than 6 passages and were frozen in multiple aliquots using freezing media (IMDM + 10% DMSO + 10% FBS).

2.2 Western blot

2.2.1 Protein preparation

To prepare protein samples for western blots, 2 or 4 million cells were pelleted, resuspended, and lysed in 75 µl ice-cold NP-40 buffer supplemented with a cOmplete protease inhibitor tablet (Roche) and incubated on ice for 1 h. 0.1 µl of Benzonase nuclease (Sigma-Aldrich) was added and samples were incubated at 37°C for 30 min. Then, 25 µl of 4x sample buffer was added and the mixture was boiled at 95°C for 5 min. If the samples were not used immediately, they were frozen at -20°C.

2.2.2 Creating gels for SDS-PAGE

10% Acrylamide running gels were made by mixing 0.5 parts each resolving buffer and acrylamide (Sigma Aldrich) with 1 part H_2O. Per 10 ml, 100 µl of APS and 10 µl of Temed were added and the running gel mixture was quickly pipetted into gel chambers. To obtain an even gel border, isopropanol was added on top. The stacking gel (1.25 ml stacking buffer, 0.625 ml acrylamide, 3 ml H2O, 50 µl APS, 5 µl Temed) was pipetted onto the running gel upon polymerization and removal of the isopropanol, before a comb was pushed into the still liquid stacking gel.

2.2.3 Coomassie blue staining

Before starting with the western blot, Coomassie staining was performed to equalize the levels of proteins in the samples. The protein samples were heated to 95°C and quickly

spun down. 5 µl of each sample were loaded as well as a prestained protein Ladder (Abcam). SDS-PAGE was run at 120V for 90 min. After that, the gel was stained for 10 min at RT with Coomassie blue. After washing with H_2O, the gel was destained in a destaining solution for 1 h, before another washing step with H_2O. The next day, the gel was imaged using a regular scanner. The necessary volume of each sample for the western blot was determined by subtracting the background from a distinct sample band in ImageJ and normalizing to the average of all samples.

2.2.4 Western blotting

For the western blot itself, the calculated amount of sample was loaded onto acrylamide gel. After SDS-PAGE, wet transfer onto a nitrocellulose membrane was performed at 4°C for 150 min at 250 mA. The membrane was blocked for 1h in, depending on the primary antibody, either 5% BSA (Sigma) or 5% skim milk (Gerbu Biotechnik GmbH) in TBST. The primary antibodies were diluted in the respective blocking solution and incubated at 4°C overnight. The next day, the membranes were washed 3x for 10 min each using TBST, before the secondary antibody, diluted in respective blocking solution, was applied and incubated for 1h at RT. After 3 washed in TBST, Abersham ECL prime detection reagent (Cytiva) was applied to develop chemiluminescence. Images were taken using the ChemiDocMP imaging system (Bio-Rad) and ImageJ was used to quantify the protein bands.

Primary antibodies: anti-$p31^{comet}$ (1:200; mouse; BSA-TBST, Sigma-Aldrich #E29.19.14), anti-CDC16 (1:500; mouse; skim-milk-TBST; Santa Cruz Biotechnology #(E-4) sc-365636), anti-α-Tubulin (1:20000; mouse; in BSA-TBST or skim milk TBST; Sigma-Aldrich T6074). Secondary antibody: HRP-linked anti-mouse IgG (1:10,000; Cell Signaling Technology 7076).

2.3 Restriction digest of plasmids

To obtain linearized plasmids ready to ligate to sgRNAs, restriction digests were made. For the digest, 1 µl of either BbsI or BsmBI-v2 together with 1 µg of plasmid DNA, 1x NEBuffer r3.1 (BsmBI-v2) or 1x CutSmart NEB buffer (BbsI) were filled up to 50 µl with H_2O and incubated at 55°C (BsmBI.v2) or RT (BbsI) for 1 h. After that, the linearized plasmid was purified using gel electrophoresis followed by gel extraction.

2.4 sgRNA design for CRISPRa and CRISPR deletions

The sgRNA for CRISPRa (Table 5) were designed to target upstream of the transcription start site of the targeted gene. Using the help of the online tool CHOPCHOP (https://chopchop.cbu.uib.no; Labun *et al*, 2019) on the setting for designing activation guides, guides were generated. Using Cas-OFFinder (http://www.rgenome.net/cas-offinder/; Bae *et al*, 2014), analysis of potential off-targets was performed. The guides for *p31^{comet}* were designed manually. The transcription start site of the genes was determined using the USCS genome-browser (http://genome.ucsc.edu; Kent *et al*, 2002). Guides were chosen within 10-1000 nt distance to the transcription start site and off-target analysis was performed as previously.

Single-cut sgRNAs for CRISPR/Cas9 based deletion of whole chromosome arms were designed to target close to the centromere region so that all protein-coding genes were excised. Guides used for partial deletion of a chromosome arm were targeted to intergenic regions at the desired sites (Table 7). Using the online tools GuideScan2 (https://guidescan.com; Schmidt *et al*, 2022) and CRISPOR (http://crispor.tefor.net; Concordet & Haeussler, 2018), guides were chosen based on their cutting efficiency. Analysis of off-targets was performed using the Cas-OFFinder.

2.5 Preparation of sgRNA plasmids for CRISPRa and CRISPR deletions

The sgRNA plasmids were created by ligating the single guide-RNA oligos (Table 7; Table 5) into the restriction sites of either the pSpCas9(BB)-2A-GFP (PX458) plasmid (BbsI restriction site) or the GFP-Neo^R plasmid (BsmBI-v2 restriction site). For the phosphorylation and annealing of sgRNA oligos in a thermocycler, following reagents were combined: 1 µl of each sgRNA oligo fwd/rev 100µM; 1 µl of 10x T4 DNA ligase buffer (New England Biolabs), 1 µl T4 PNK (New England Biolabs) and 6 µl H_2O. The thermocycler protocol was the following: 37°C, 30 min; 95°C, 5 min; -1°C/30 sec to 25°C. To ligate the plasmids with sgRNA oligos for 1 h at RT, 50 ng of either BbsI or BsmBI-v2 (New England Biolabs) digested plasmids were combined with 1 µl of 1:200 diluted the phosphorylated and annealed oligo duplex, 1 µl 10x T4 DNA ligase buffer, 1 µl T4 DNA Ligase (New England Biolabs) and filled to 10 µl with H_2O. The ligated plasmid was then transformed into DH5alpha *E. coli*. After thawing the competent bacteria from -80°C on ice for 10 min,

10 µl of the ligation was added and incubated for 30 min on ice, followed by a 45 s heat shock in a 42°C waterbath. After 2 min on ice, the bacteria were streaked out on preheated AMP-plates, and the bacteria incubated at 37°C overnight. To make sure that the sgRNA was successfully ligated into the transformed plasmids, colony PCRs were performed for some of the colonies. After confirming the sgRNAs were in the plasmid, the confirmed colonies were picked and expanded into LB-AMP (100 µg/ml) liquid cultures, which were incubated shaking overnight at 37°C.

2.6 Colony polymerase chain reaction (PCR)

To confirm the successful ligation of plasmids with sgRNAs, PCRs of single colonies were done to check for the insertion. Single colonies were picked using a 200 µl pipette tip and mixed into a PCR-mastermix, which contained 1x Phusion HF Buffer (Thermo Fisher Scientific), 0,4 µl of 10mM dNTPs (New England Biolabs), 1 µl of 10 µM forward and reverse primer (Microsynth), 0.2 µl of Phusion polymerase and H_2O to a total volume of 20 µl. The following thermocycler program was used: Activation and denaturation at 98°C for 30 sec-1 min, 34 cycles of denaturation at 98°C, annealing at 55-62°C for 30 sec, depending on the annealing temperature of the primers, elongation for 30 sec-2 min, depending on fragment size, at 72°C followed by a final extension step at 72°C for 5 min. The obtained PCR fragments were then checked for the correct size using gel electrophoresis.

2.7 Agarose gel electrophoresis

For visualization of PCR products, 0.8% agarose gels were dyed with peqGREEN (VWR), while purification required 0.8% agarose gels stained with crystal violet. For size comparison, a 1 kb Plus DNA ladder (New England Biolabs) was loaded. To load the samples, a 6x Orange G loading dye was used. The gels were run for 30 min at 90V and examined using a Gel DocTM XR+ system (Bio-Rad).

2.8 Gel extraction

After purifying linearized plasmids using agarose gel electrophorese, they were subsequently extracted from the gel using the QIAquick® Gel Extracton Kit (QIAGEN). For that, the bands were excised from the gel, the slices weighted and 3 volumes of QG buffer were added. After 10min incubation in a shaking 50°C thermomixer (Eppendorf) to

dissolve the gel slice, 1 volume isopropanol was added and up to 800 µl were transferred to a spin column. The sample was spun down for 1 min at max speed or 20000 x g in a tabletop centrifuge and the flow-through was discarded. The sample was then washed using 750 µl of PE-buffer and centrifuged for 1 min at maximum speed. To dry the column, it was centrifuged for 3 min at full speed. After transferring the column to a new 1.5 ml reaction tube, 20-50 µl of H_2O were applied to the matrix. After incubating for 1min, the DNA was eluted by centrifuging for 1 min at full speed.

2.9 Plasmid minipreparation

To obtain the plasmid from bacterial liquid cultures, plasmid mini preps were done using the instructions from QIAprep Spin Miniprep Kit (QIAGEN). In short, the bacteria from liquid cultures were pelleted in a 2 ml reaction tube by centrifuging at 14.000 rpm for 2 min. After the supernatant was discarded, the pellet was resuspended in 250 ml buffer P1. The cells were lysed by adding 250 µl buffer P2 followed by 350 µl N3 buffer, after which the sample was inverted and centrifuged for 10 min at 14.000 rpm. The supernatant was transferred to a spin column and, after 1 min rest, centrifuged for 2 min at 8.000 rpm, followed by a washing step with 750 µl of buffer PE and centrifugation for 1 min at 8000 rpm. The membrane of the spin column was dried by centrifuging at maximal speed for 1 min. 50 µl of H_2O were added to the column, before resting for 3-5min.The DNA was eluted by 1 min centrifugation at full speed.

2.10 Generation of deletion cell lines

To generate cell lines that lost chromosomes, sgRNA targeting different chromosome arms were designed und ligated into Cas9-expressing PX458 plasmid. The plasmid was transfected into selected HAP1 or dipHAP1 cell lines using XtremeGene HP (Sigma-Aldrich). Per well of a 6-well plate, 1 µg of plasmid-DNA was mixed with 100 µl of Opti-MEM (Gibco), before 1 µl of XtremeGene HP was added. After 15 min incubation at RT, the mixture was added dropwise to the cells. 48 h after transfection, cells were FACS-single cell sorted for presence of Cas9 protein (GFP-positive). Approximately 10 days following the SCS, clonal colonies were expanded into 12-well plates. Once confluent, half of the cells were gDNA prepped for qPCR, while the other half was further cultivated.

2.11 Genomic DNA preparation

To check the genotype using qPCR, a quick genomic DNA-prep was used. For that, a suspension of (dip)HAP1 cells in PCR tubes was spun down using a small tabletop centrifuge for ~30 min or until a pellet has formed. The supernatant was removed, and the pellet resuspended in 50 µl of 0.5x direct lysis buffer (10 mM Tris pH 8.0, 2.5 mM EDTA, 0.2 M NaCl, 0.15% SDS, 0.3% Tween-20). The following thermocycler protocol was then used: 65°C, 30s; 8°C, 30s; 65°C, 1.5 min; 97C, 3 min; 8°C, 1 min; 65°C, 3 min; 97°C, 1 min; 65°C, 1 min; 80°C, 10 min. The obtained product concentration was then measured using the Qubit dsDNA HS assay (Invitrogen) and used for qPCR without further purification.

For a higher yield of product and for sequencing the QIAamp UCP DNA micro Kit (QIAGEN) was used for gDNA prep. In short, a cell pellet was resuspended in 50 µl 1x PBS before addition of 50 µl AUT buffer. After Addition of 10 µl Proteinase K, 100 µl of buffer AUL were added, samples vortexed for 15 seconds and subsequently incubated shaking at 56°C for 10 minutes. To remove any drops, samples were quickly centrifuged. 50 µl of 100% EtOH were added to the lysate, pulse-vortexed for 15 s and incubated for 3 min at RT. The samples were centrifuged at 8000 rpm for 1 min and the flow-through discarded. The membrane was dried by centrifugation at full speed for 3 min. The spin column was transferred to a new 1.5 ml reaction tube and 50 µl of H_2O were added to the center of the spin column. After 5 min incubation at RT, the DNA was eluted by centrifugation at full speed for 1 min.

2.12 Assessing aneuploidy using quantitative PCR (qPCR)

To confirm gains and losses of chromosomes, we performed qPCRs using genotyping primers targeting either centromere or telomere regions as listed in Table 4 or Albumin. 1 µl of 10 ng sample DNA was mixed with 10 µl Luna qPCR master mix (New England Biolabs) and 8 µl of H_2O. Forward and reverse primers were diluted 1:40 with H_2O from 100 µM stock and 1 µl of primer mix was added per sample. All samples were applied in triplicates. Additionally, to the samples, negative controls without DNA to detect contamination of the reagents were added in triplicates per primer-pair. On every plate, a euploid WT (either haploid or diploid HAP1) sample and a positive control for of the gained

chromosome was applied. qPCRs were performed in 96-well plates (Eppendorf; Bio-Rad), which were spun down after adding a clear heat-seal. The qPCR reactions were performed using the Mastercycler epRealplex from Eppendorf. The qPCR program for all qPCRs was the following: An initial 95°C activation step for 5 min was followed by 35 cycles of denaturation at 95°C for 15 sec, annealing at 63°C for 40 sec and elongation at 72°C for 10 sec, followed by a 20 min melting curve analysis with temperatures increasing to 95°C. The obtained cycle threshold Ct-values were normalized to the euploid WT sample and albumin was used as a reference gene. Additional to the qPCR analysis, the karyotype of most samples was verified using the Illumina Next generation whole-genome sequencing technique and analysis performed as previously stated in Adell & Klockner *et al*, 2023.

2.13 Colony formation assay

To determine growth with and without reversine via the formation of colonies grown from single cells, 600 cells were seeded into 6-well plates either supplemented with 300 nM (dipHAP1 cells) or 250 nM (HAP1 cells) reversine (+Rev) or the according amount of DMSO (-Rev). The cells were incubated for 12 days, after which they were fixed for 20 min in 4% formaldehyde (Thermo Fisher Scientific) in PBS, followed by a wash-step using PBS. Next, the colonies were stained with Crystal Violet before washing with H_2O 2-3 times. After the plates were dried, they were imaged using the Bio-Rad ChemiDocMP imaging system. Colony formation was analyzed using ImageJ by measuring the area above a threshold that was determined for the whole plate.

2.14 DNA staining and live-cell imaging

About 2 days before starting the microscopy, cells were seeded in 6- or 12-well plates with glass bottoms (Cellvis) to reach a final confluence of about 60-80%. 3h before the imaging, cells were stained using 125 nM Spy650-DNA or SiR-DNA (Spirochrome). During the imaging process, the media was exchanged for Opti-MEM containing 12.5 nM of the respective DNA-stain and, when labeled in the figures, 400 nM (dipHAP1) or 350 nM (HAP1) of reversine was added. The automated live-cell microscopy was perfomed using a 50x water immersion objective and a 0.5x zoom lense on a Celldiscoverer 7 screening microscope (Zeiss). During the course of the experiment, cells remained in 37°C at 5%

CO_2. 3-dimensional time series with a duration of 2.5 h were recorded, during which pictures of the cells were taken every 3 min using the Zeiss Zen 2.5 software.

2.15 Flow cytometry for DNA content analysis

To determine the ploidy of HAP1 cells, they were trypsinized and stained in ~500 µl PBS+10% FBS with 1 µl of Hoechst33342 (Thermo Fisher Scientific). After 30 min incubation, the flow cytometry was done using a FACSAria IIu cell sorter (BD) with an argon laser in the UV range. As controls, both haploid and diploid HAP1 WT samples were used.

2.16 Fluorescence-activated cell sorting (FACS)

Sorting of cells was performed on a FACSMelody cell sorter (BD). Cells were trypsinized and suspended in PBS supplemented with 10% FBS. Cells were either bulk sorted into Falcon-tubes, or into single-cell sorted into 96 well plates. To suppress growth of any contaminants, the media was supplemented with Normocin (Fisher Scientific) after FACS. For cell lines being sorted for GFP expression, a laser with wavelength of 488 nm was used, while cells sorted for mCherry were excited at 561 nm wavelength.

2.17 Lentiviral transduction

To obtain dipHAP1 cell lines expressing dCas9-VPR-mCherry for CRISPR-activation, HEK293HiEx cells were transfected using XtremeGene9 (Roche) with the dCas9-VPR-mCherry expression plasmid, a po882 packaging plasmid and a pMD2.G VSV-envelope plasmid in a ratio of 5:5:1. 15 µl XtremeGene9 were mixed with 500 µl Opti-MEM, incubated for 5 min at RT before 4082 ng dCas9-VPR-mCherry plasmid, 4082 ng po882 plasmid and 816 ng pMD2.G plasmid (Table 10) were added. After another 15 min incubation at RT, the mixture was added dropwise to HEK293HiEx cells in a 10 cm dish. 3 days later, the supernatant containing the virus was filtered through a 0.45 µm filter. Target cells were transduced with a 1:1 dilution of virus and media. After 3 days incubation, the cells were washed to get rid of excess virus and FACS single-cell sorted for mCherry. After ~10 days, single colonies were expanded in 12-well plates. mCherry fluorescence was measured using flow cytometry and cell lines stably expressing mCherry after about 10 days were selected.

2.18 Gibson cloning of a p31^{comet} sgRNA plasmid

For overexpression of *p31^{comet}*, a GFP-Neo^{R} plasmid was designed containing 3 different sgRNAs in succession each with their own hU6 promoter. Four fragments were generated via PCRs, primers and templates are listed in Table 6, and subsequently extracted from an agarose gel. The Gibson assembly was done using approximately equimolar amount of each fragment, altogether 2.5 µl, and mixing with 2.5 µl Gibson assembly master mix. After incubation at 50°C for 1 h, it was transformed into DH5alpha *E. coli*, grown overnight, transferred into liquid cultures overnight and plasmid mini-prepped to obtain the assembled plasmid.

2.19 CRISPRa overexpression

2.19.1 Transfection and selection

To induce overexpression of target genes, the cell lines expressing dCas9-VPR-mCherry were transfected with sgRNA GFP-Neo^{R}-expressing plasmids using XtremeGene9. Guides on the plasmid targeting the promotor of target genes are listed in Table 5. To overexpress *p31^{comet}*, either 3 guides were transfected simultaneously, or a plasmid generated by Gibson cloning containing the 3 p31^{comet} sgRNAs was used. As control, cells were transfected with the empty vector not containing a sgRNA sequence. Cells that expressed plasmid were selected for using 1.5-2 mg/ml G418/Geneticin for at least 5 days. After that, either mitotic timing was measured as described or the cells were pelleted for RNA extraction and subsequent RTqPCR.

2.19.2 RNA isolation

The RNA of pelleted cells was isolated using the RNeasy Mini Kit (QIAGEN). A maximum of 1x10^7 cells were pelleted and 600 µl of buffer RLT was added, supplemented with 40 µl 1M DTT per ml RTL buffer. After intensely vortexing the cells, 1 volume of 70% EtOH was added to the lysate and mixed by pipetting up and down. Up to 700 µl of the sample were transferred to a spin column, centrifuged for 15 s at 10000 rpm and the flow-through discarded. 700 µl of buffer RW1 were added before repeating the centrifugation step. 500 µl of buffer RPE was added, centrifugation and flow-through discarding were repeated, before finally adding 500 µl buffer RPE to the column and centrifuging for 2 min at 10000 rpm. The sample was placed in a new collection tube and the column centrifuged dry for

1 min at full speed. The column was placed in a new 1.5 ml reaction tube, 30-50 µl of RNase-free water was added to the membrane and after 5 min at RT, the RNA was eluted by centrifuging at 10000 rpm for 1 min.

2.19.3 DNase I treatment

To get rid of residual DNA, RNA samples were treated with RNase-free DNase I (New England Biolabs). On ice, 10 µg of RNA, 10 µl of 10x DNase I reaction buffer (New England Biolabs), 1 µl or 2 Units of DNase I and H_2O up to 100 µl were incubated at 37°C for 10 min, before 1 µl 0f 0.5M EDTA were added. The DNase was heat-inactivated at 75°C for 10 min.

2.19.4 Reverse transcription

Before RTqPCR, the RNA had to be reverse transcribed into cDNA. First, up to 1 µg of RNA samples and 2 µl 50 µM oligo d(T)23 VN (New England Biolabs), 1 µl of 10 mM dNTPs and nuclease free H_2O up to 10 µl were mixed and denatured at 65°C for 5 min, before putting on ice. Following components were then added: 4 µl of 5x ProtoScript II buffer, 0.1M DTT, 1 µl of ProtoScript II Reverse Transcriptase (all New England Biolabs), 0.2 µl of RNase ribonuclease inhibitor (Promega) and 2.8 µl of H_2O. The 20 µl cDNA reaction was incubated for 1 h at 42°C, before the RT was inactivated for 20 min at 65°C. The concentration of the synthesized cDNA was measured using the Qubit dsDNA HS assay (Invitrogen). To generate the cDNA for RTqPCR for *TTN*, the TTN-RTqPCR primers (Table 8) were used instead of the oligo d(T).

2.19.5 Reverse transcription quantitative PCR (RTqPCR)

The cDNA samples were diluted to the same concentration (4-8ng/µl) for RTqPCR. The same protocol as for the standard qPCR as already described was used. GAPDH was used as a reference gene. All RTqPCR primers used are listed in Table 8.

2.20 Scratch assay

For the scratch assays, around 1-1.5 Mio cells were seeded in 12-well plates and grown 1-2 days until almost 100% confluent. All cell lines were seeded in duplicates. The monolayer was then scratched two times perpendicular to each other using a 200 µl pipette tip and the media was exchanged for serum-reduced media (IMDM+1% P/S +

0.1% FBS). Images were taken using the EVOS M5000 Imaging System microscope (10x magnification objective). Immediately after the scratch (0h), after 24 and 48 hours, respectively, pictures of the same area were taken for every cell line. Analysis of the distance between the scratch edges was manually done for 5 different random points per image using Fiji (ImageJ). To compare the growth of different cell lines independently of the initial scratch width, a normalized closing rate was calculated by dividing scratch width after 0h by the remaining distance between edges at 48h and normalizing to WT.

2.21 Statistical analysis

Most experiments were repeated 2 or more times. The indicated number n in graphs indicates biological replicates. In colony formation assays, the number of points per bar graph represents the value per one replicate, apart from WT data, which always has 3 replicated values. In qPCRs, the number of points represents the number of experiments with 3 replicates each. Analysis was performed using the GraphPad Prism software, version 8.0.1. Statistical differences between 2 cell lines were determined using the unpaired student's t-test, while differences between more than 2 cell lines were done using ANOVA multiple comparison. Which test was used is an experiment is indicated in the figure legends beneath. The standard deviation (+/-SD) is represented by the error bars. For either ANOVA or unpaired student's t-test: (∗) $P \leq 0.05$, (∗∗) $P < 0.01$, (∗∗∗) $P < 0.001$, (∗∗∗∗) $P < 0.0001$, (ns) not significant, $P > 0.05$.

3 RESULTS

3.1 CRISPRa

3.1.1 p31^{comet} and CDC16 protein levels are decreased in aneuploid cell lines

The first aim of my master thesis was to further uncover the role of *p31^{comet}* and *CDC16* via overexpression in cell lines heterozygous for those genes. For this, I measured protein levels of engineered cell lines which were used as parental cell lines in further experiments. Those were the following dipHAP1 (dH1) cell lines: WT, 6p full del. 2, 13q full del and CDC16 +/-**.** To verify that those monosomies and deletion cell lines had an impact on p31^{comet} and CDC16 protein levels, I performed western blot analysis (Figure 3). As a loading control, alpha tubulin antibodies were used, and the expression levels were normalized against WT. Indeed, as expected, the blots show that the levels of p31^{comet} were decreased about 50% for the engineered chromosome 6p monosomy cell line compared to WT. The CDC16 expression levels in the chromosome 13q monosomy and CDC16 heterozygous KO cell lines were also decreased, with 40% and 26% respectively, compared to WT levels. Put together, I was able to show that the protein abundance of p31^{comet} and CDC16 was approximately proportional to their copy number.

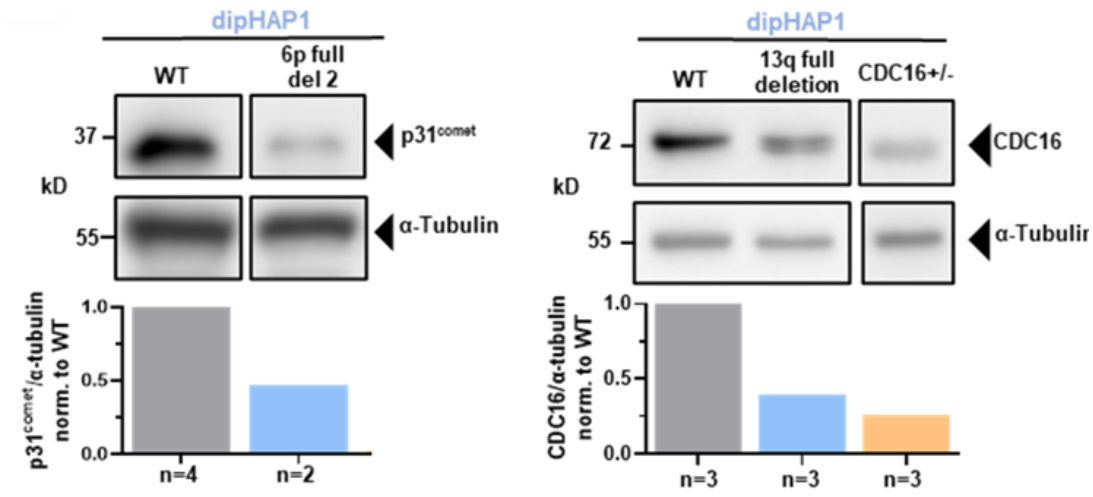

Figure 3: Western blots of p31^{comet} and CDC16 protein levels. Alpha-tubulin was used as the loading control, intensity of proteins of interest was normalized to WT, respective n-values are listed underneath.

3.1.2 Establishing a CRISPRa system leading to overexpression of target genes

Now that the decreased protein levels of p31^{comet} and CDC16 were confirmed in the tested cell lines, I aimed to overexpress those genes to further strengthen their role in reversine resistance and mitotic timing. We decided on a CRISPRa (CRISPR activation) approach, that relies on bringing activators to the promoter of target genes to overexpress them (Figure 4; Perez-Pinera *et al*, 2013). To achieve this, a catalytically dead Cas9 (dCas9) protein coupled to transcriptional activators and a short guide RNA, that leads the dCas9 to the target DNA sequence, are needed. Such a transcriptional activator can be a tripartite fusion of VP64, p65 and Rta, or short VPR (Chavez *et al*, 2015).

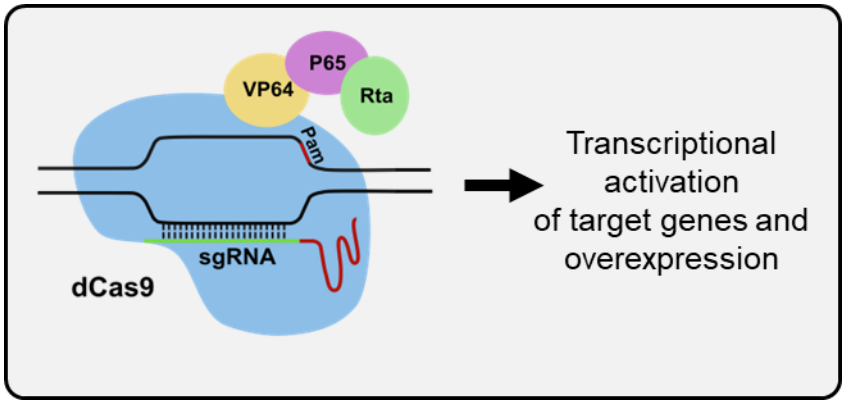

Figure 4: Schematic representaion of dCas9-VPR for CRISPRa.

Our approach was to generate cell lines constitutively expressing a plasmid containing a dCas9-VPR fusion protein with a P2A-linked mCherry marker (dCas9-VPR-mCherry), while the sgRNA would be delivered over a separate plasmid (Figure 5A). The dCas9-VPR-mCherry expression plasmid together with envelope and packaging plasmids were used to generate lentivirus in HEK293HiEx cells. Using this virus, parental dipHAP1 cells (WT, 6p full del. 2, 13q full del. and CDC16+/-) were transduced. After FACS single cell sort and clonal expansion, expression of the mCherry protein was checked via flow-cytometry over a span of at least 10 days to obtain clonal populations with stable expression (Figure 5A, B). While the dCas9-VPR-mCherry WT (hereinafter referred to as dCas9-VPR-WT), the dCas9-VPR-6p full del 2 (dCas9-VPR-6p) and the dCas9-13q full del (dCas9-VPR-13q) cell lines showed low to moderate expression of mCherry, the dCas9-VPR-CDC16+/- was a high expressing cell line. The karyotypes of those cell lines were confirmed via Illumina next-generation sequencing (Figure 5C) and remained similar to their parental cell lines (Supplemental Figure 3), however, small changes were

observed for all but the dCas9-VPR-CDC16+/- cell line. The dCas9-VPR-WT cell line remained almost euploid, but had a partial X gain, while the 13q full deletion had an Xq loss. The dCas9-6p cell line had partial gains and losses of chr. 17 and a loss of chromosome Xp. Partial chr. 15 gain is intrinsic to this cell line.

To confirm that the CRISPRa system worked, different sgRNAs (Table 5) in a GFP-Neo^R vector backbone were transfected into the dCas9-VPR-WT and selected for at least 5 days using G418.This was to make sure only cells that incorporated the plasmid survived. As control, the empty GFP-Neo^R vector was transfected. For *p31^{comet}* overexpression, either all three guides were transfected simultaneously (p31 3x sgRNA) or a Gibson GFP-Neo^R vector was used containing all 3 guides on one plasmid (p31 Gibson sgRNA). As a control for the CRISPRa overexpression system, a guide for the gene *TTN* was used, which should normally not be expressed in dipHAP1 cells. The expression levels of the genes of interest were tested via their RNA level in RT-qPCRs (Figure 5D). As a reference gene, *GAPDH* was used.

As expected, the *TTN* guide led to increased levels of *TTN* expression. Compared to empty vector, sgRNA p31-3x and p31-Gibson showed elevated expression levels of *p31^{comet}* and the CDC16-sgRNA C1 increased levels of *CDC16* RNA, even though the standard deviations were very high. The parental cell lines 6p full del 2, CDC16 +/- and 13q full del as controls showed decreased RNA levels for *p31^{comet}* and *CDC16*, respectively. However, while the dCas9-VPR cell lines had undergone transfection and extensive selection, possibly leading to accumulation of mutations or changes in baseline gene expression levels, the parental cell lines did not. Nevertheless, the results show that I was able to successfully establish a CRISPRa overexpression system in dipHAP1 dCas9-VPR-WT cells.

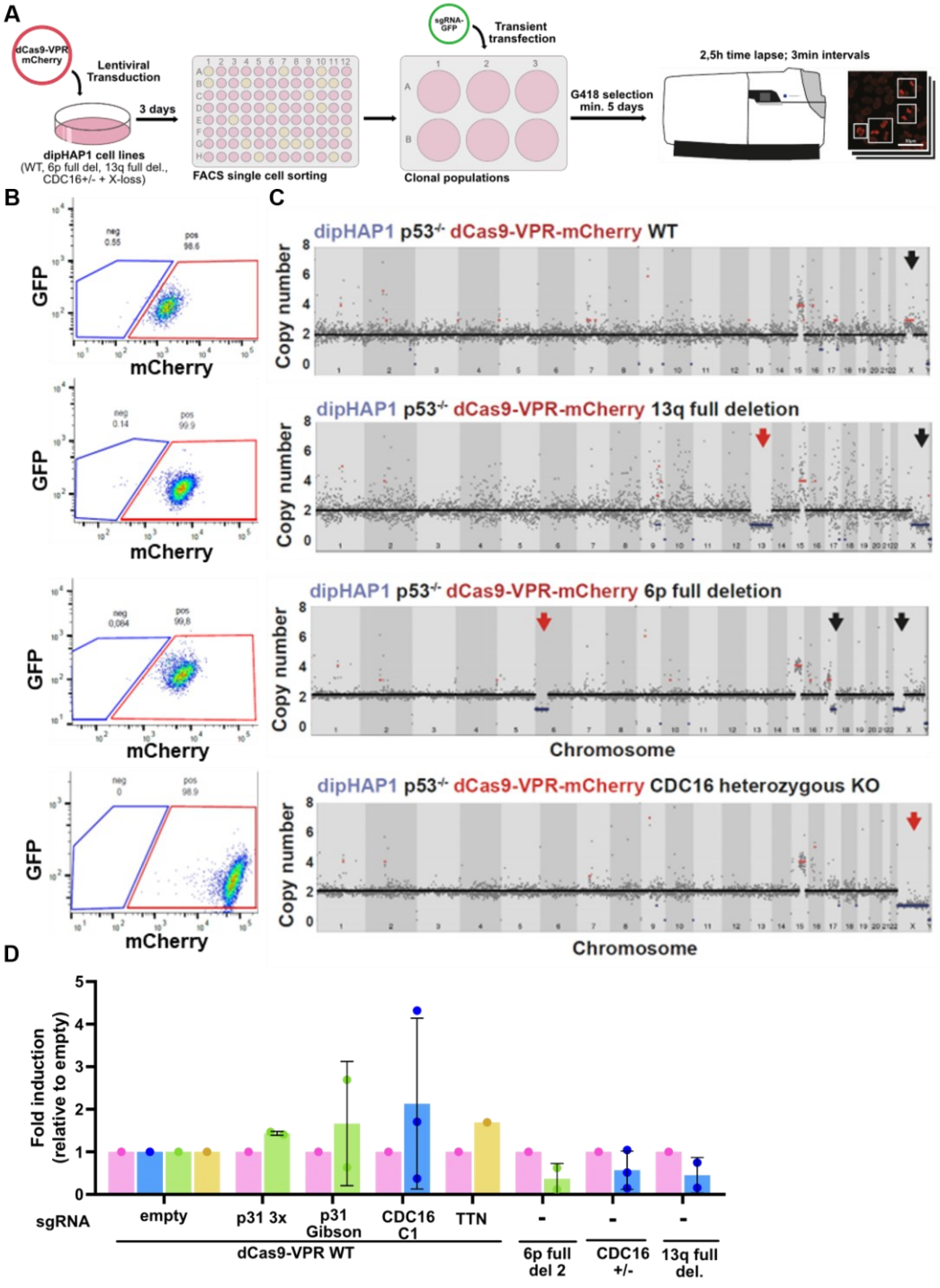

Figure 5: CRISPRa approach. (A) General approach for overexpression of target genes using the CRISPRa system, adapted from Adell & Klockner et al, 2023. (B) Flow cytometry results for mCherry expressing cell lines depicted in (C). (C) Copy number profiles of dCas9-VPR-mCherry expressing cell lines. Blue dots represent losses, red dots represent gains.Chr. 15 gain is intrinsic for dipHAP1 cells. (D) RTqPCR results for testing different sgRNAs in dCas9-VPR-WT to induce overexpression as indicated by fold induction. GAPDH was used as a reference gene, all values were normalized to WT.

3.1.3 Overexpression of p31^{comet} and CDC16 is sufficient to decrease mitotic delay

As previously established, dipHAP1 cell lines heterozygous for either *p31^{comet}* or *CDC16* rescue growth in reversine and extended mitotic timing (Adell & Klockner *et al*, 2023). After determining that the sgRNAs increased RNA levels in dCas9-VPR-WT, the next step was to show that the CRISPRa system was able to eliminate the phenotype of the parental cell lines heterozygous for *p31^{comet}* and *CDC16* in the mitotic timing.

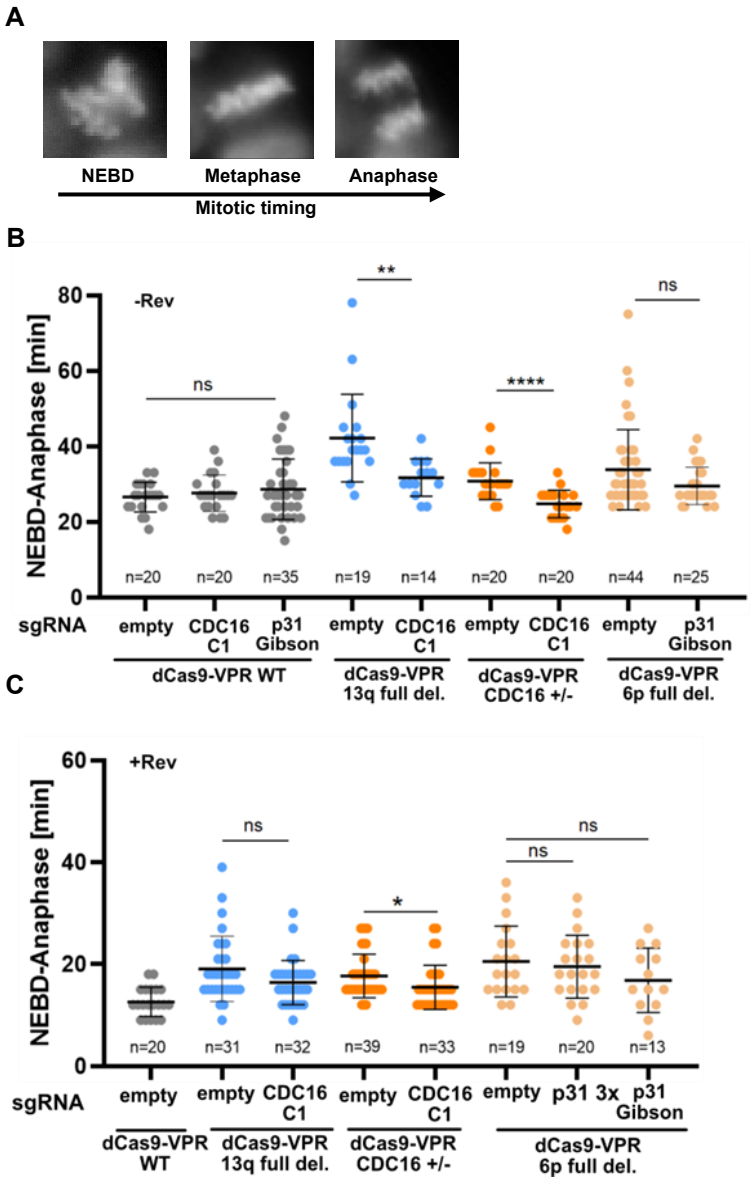

Figure 6: Change in mitotic timing after CRISPRa. (A) Mitotic timing measurement from NEBD to Anaphase. (B) Duration of NEBD-Anaphase in dCas9-VPR cell lines without reversine and (C) with reversine. n= indicated below graphs. The bars represent the +/- SD value. P-values were obtained through unpaired students t-tests.

To achieve that, I transfected cell lines with the different sgRNAs, selected for a minimum of 5 days in G418 and the unsynchronized populations were live-cell imaged after staining with SiR-DNA. To ensure only cells with the sgRNA-GFP-plasmid were analyzed, an additional picture in the GFP channel was taken to selectively analyze only GFP positive cells in which transfection of the sgRNAs was successful. The mitotic timing was assessed by measuring the interval from nuclear envelope breakdown (NEBD) to anaphase (Figure 6A).

Our hypothesis was, that, while deletion of *p31^{comet}* and *CDC16* lead to a delay in anaphase (Figure 2B), overexpression should revert the timing back to WT level. In the absence of reversine, the mitotic timing for dCas9-VPR-WT remained consistent at ~28 min, regardless of whether an empty vector, CDC16-sgRNA or p31-Gibson were introduced (Figure 6B). This suggests that neither expression of *p31^{comet}* and *CDC16* exceeding WT levels or the plasmids themselves changed the mitotic timing phenotype.

Excitingly however, in the monosomic dCas9-VPR-13q cell line, addition of the CDC16-sgRNA led to a significant 10 min decrease in mitotic timing. Similarly notable results were observed in the dCas9-VPR-CDC16+/- cell line, were the addition of CDC16-sgRNA significantly reduced timing from ~31 min to ~25 min. In the 6p monosomic cell line, addition of the p31-Gibson sgRNA rescued the anaphase delay, reducing timing by almost 5 min to ~29.5 min. Addition of reversine (Figure 6C) yielded similar intriguing results. The mitotic timing of dCas9-VPR-WT with empty vector drastically decreased timing to ~13 minutes. A reduction of mitotic duration by ~3 min was achieved in both dCas9-VPR-13q and dCas9-VPR-CDC16+/- upon addition of the CDC16-sgRNA compared to empty. Furthermore, for the monosomic dCas9-VPR-6p cell line addition of both the 3x p31 guides and p31-Gibson slightly decreased delay in anaphase in presence of reversine compared to empty vector, with 1 min and 3 min reduction, respectively. It is worth noting, that even with the addition of sgRNAs, the mitotic timing in monosomic cell lines did not quite reach the levels of dCas9-VPR-WT. This indicates, that *CDC16* and *p31^{comet}*, while being significant contributors to the observed phenotype, maybe are not the sole genes on their respective chromosome responsible for these effects.

Overall, these results confirm firstly, that *CDC16* and *p31^{comet}* indeed play a pivotal part in modulating mitotic timing, both in presence and absence of reversine. Secondly, those experiments confirm the functionality of CRISPRa induced overexpression in live-cell experiments as overexpression of both genes resulted in the reduction of mitotic duration.

3.1.4 Experimental evaluation of CRISPRa system using RTqPCR in CDC16- and p31^{comet} heterozygous cell lines

Following the successful implementation of the CRISPRa system in live-cell imaging experiments, we wanted to determine expression levels of *CDC16* and *p31^{comet}* in the dCas9-VPR-expressing 6p, 13q and CDC16+/- cell lines through RTqPCR.

In comparison to WT empty control, the monosomic cell lines dCas9-VPR-6p empty exhibited reduced expression levels of *p31^{comet}*. Both the addition of sgRNA p31-3x and p31-Gibson in dCas9-VPR-6p resulted in and approximate duplication of *p31^{comet}* expression compared to empty vector. However, the achieved expression did not fully restore to the levels observed in the dCas9-WT+ empty, plateauing at a level similar to the parental dipHAP1 6p full del 2. This discrepancy might be attributed to generally lower *p31^{comet}* expression in the dCas9-VPR-6p cell line. Nonetheless, the overexpression, relative to empty vector, appeared successful (Figure 7A).

Contrarily, in dCas9-VPR-13q, transfection with CDC16-sgRNA C1 led to an apparent decrease of RNA levels compared to empty, leading to *CDC16* levels falling even below those in the parental cell line (Figure 7B). The expression of *CDC16* in dCas9-CDC16+/- with empty vector was approximately twice as high as in dCas9-VPR-WT+emtpty. However, *CDC16* levels remained the same after addition of the CDC16-sgRNA (Figure 7C).

Although these results do not consistently align with the initially observed overexpression in dCas9-VPR-WT and the findings from the mitotic timing experiment, it is of not that some measurements exhibited a high standard deviation, potentially compromising reliability. This variability may stem from issues during the RTqPCRs. Inconsistencies in Ct values for *GAPDH* across different experiments, even within the same cell line (Table 11), may be attributed to the method of selecting transfected cells in the antibiotic G418 for at least 5 days, possibly resulting in gene expression changes. Cultivation for longer

periods of time also leads to loss of the resistance plasmid over time as it is not replicated, resulting in reduced sgRNA expression.

In summary, the overexpression of *CDC16* and *p31^{comet}* RNA levels was not conclusively demonstrated. However, transfection of dCas9-VPR-WT cell lines with the CDC16- and p31^{comet}-sgRNAs did not decrease mitotic timing (Figure 6B). This suggests that the reduction of timing in the engineered cell lines was not a random effect of the plasmid, but the desired overexpression of *p31^{comet}* and *CDC16*. The RTqPCR setup may have introduced unexpected variables. While the experimental outcomes did not clearly validate the expected overexpression of *CDC16* and *p31^{comet}* RNA levels, the phenotypic changes in mitotic timing underscore the effectiveness of the CRISPRa system. *CDC16* and *p31^{comet}* are important in the modulation of mitotic timing and these results contribute to understanding the role of those genes in reversine resistance.

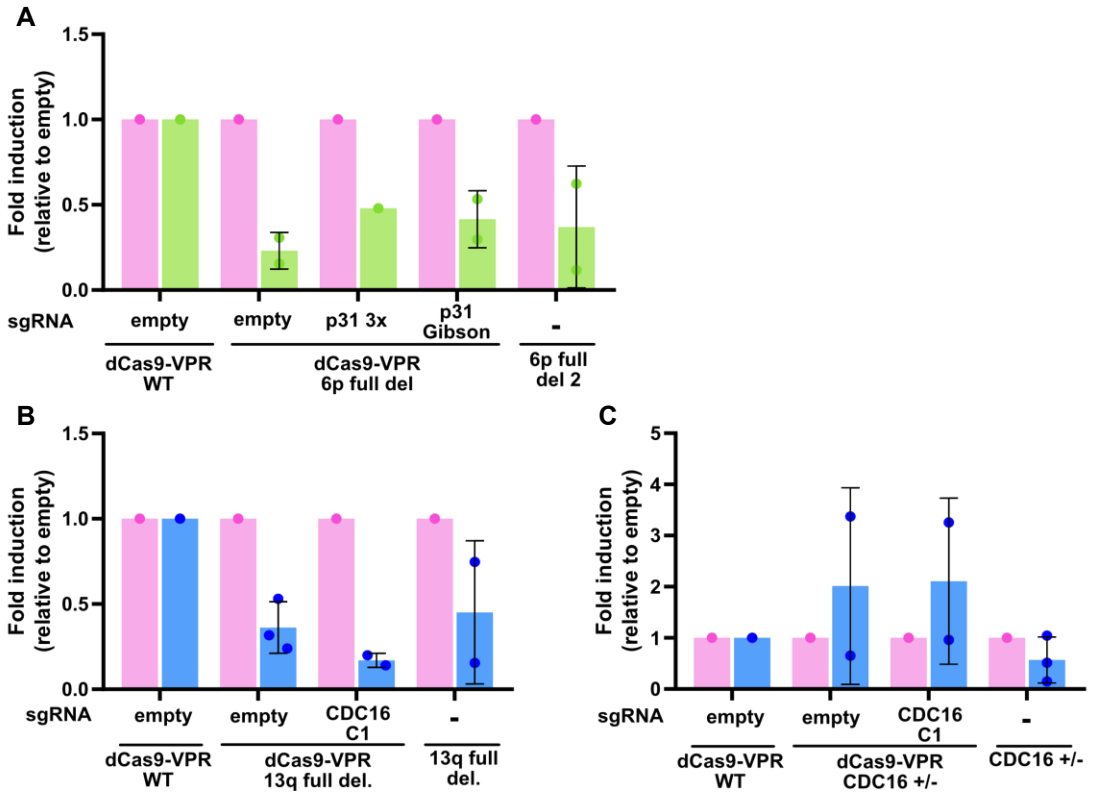

Figure 7: CRISPRa in CDC16- and p31^{comet}-heterozygous cell lines. (A, B, C) RTqPCR results for different p31^{comet} guides, CDC16 C1 sgRNA and empty sgRNA in dCas9-VPR-6p, dCas9-VPR-13q and dCas9-VPR-CDC16+/- to induce overexpression as indicated by fold induction, normalized to WT. Reference gene was GAPDH. n=indicated by points in bar graphs. The bars represent the +/- SD value.

Loss of whole chromosome (arms) can be beneficial for growth under specific circumstances and single genes can offer selective benefits. Like chromosome losses, reoccurring gains of chromosomes were found after adaptation to reversine (Adell & Klockner *et al*, 2023). We then sought to determine the basis behind gain of those specific chromosomes and whether gain of chromosomes can offer similar advantages to chromosome losses.

3.2 Chromosome gains

3.2.1 Identifying cell lines with specific chromosome gains

As mentioned before, adaptation of different cell lines in reversine led to accumulation of cell-type and cell-line specific aneuploidy patterns. As some losses have already been the subject of extensive studies (Adell & Klockner *et al*, 2023), we then focused on chromosome gains. To elucidate the effects of chromosome gains on reversine resistance, we choose different adapted cell lines with chromosome gains of interest, which for us were gains of chromosome 1, 5 and 8. Those chosen cell lines were then cultured in standard culture media. We picked 4 haploid HAP1 and 3 diploid dipHAP1 cell lines collected after 30 or 60 days of reversine adaptation, respectively, to conduct further experiments (Figure 8A). HAP1 cells were chosen, as their haploid karyotype hinders them from losing chromosomes, making them ideal to study gains. HAP1 4F and dipHAP1 #14 were chosen to study gain of chromosome 1, HAP1 4C, 1D and dipHAP1 #11 to study gain of chr. 8, HAP1 2C to investigate combined gain of 1 and 8 and dipHAP1 #4 to look at chr. 5 gains. After cultivating those 7 cell lines (HAP1 4F, 4C, 1D, 2C and dipHAP1 #11, #4 and #14) for approximately 2 weeks under standard conditions, an initial gDNA-qPCR was done to check for the gain of the chromosomes we were most interested in (Figure 8B). Through this, we were able to obtain cell lines with gains of chromosomes 1q, 8q, 5p and a combined gain of 1q and 8q. Partial gain of chr. 15 is intrinsic for both HAP1 and dipHAP1 cells.

All those cell lines were subsequently FACS single-cell sorted, clonal populations were grown and karyotyped using qPCRs (Supplemental Figure 4). Candidate cell lines were subsequently whole-genome sequenced using Illumina next-generation sequencing (Supplemental Figure 8). We ascertained the ploidy of the haploid cell lines via staining with Hoechst and flow cytometry (Supplemental Figure 10).

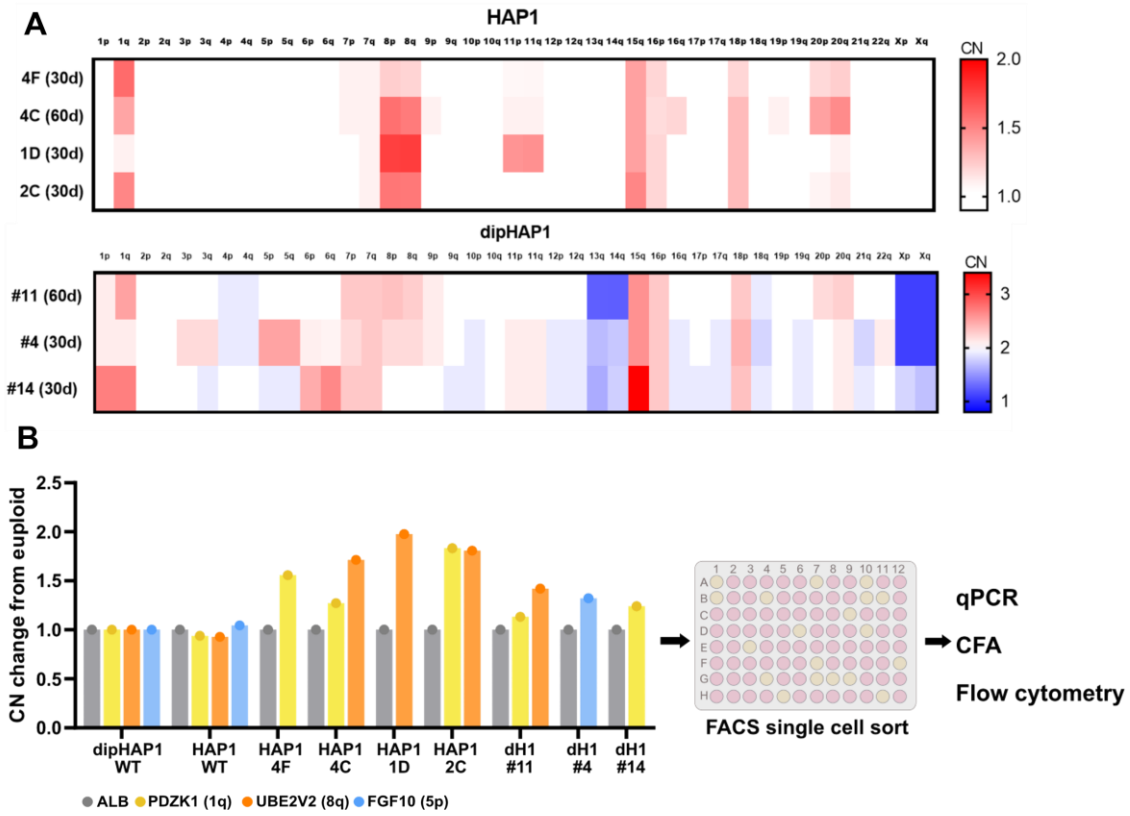

Figure 8: Identifying cell lines with chromosme gains of interest. (A) Heat maps depicting the change in copy numbers (CN) of chromosomes in HAP1 and dipHAP1 cell lines, names and duration of adaptation indicated on the left. 30d: 30days adapatation to reversine, 60d: 60 days adaptation; Partial gain of chr. 15 is cell line instrinsic. (B) qPCR results for chosen cell lines idnetifying gains of chromosomes, normalized to WT.; reference gene was *GAPDH*, n=1, and further approach.

3.2.2 Growth data in HAP1 cell shows that chromosome gains can confer resistance to reversine

After determining the karyotype of different clonal HAP1 cell lines, we tested their growth using colony formation assays. If the gain of a certain chromosome would grow better under reversine, obtaining and retaining such a gain during the adaptation process would likely not be a random event. The data for HAP1 cell line 1D can be found in Supplemental Figure 1 and CFAs for additional cell lines can be found Supplemental Figure 5.

Table 1: Karyotype of indicated cell lines as identified by Illumnina sequencing or qPCR (n.s.= not sequenced).

Cell line (Name)	Karyotype	Cell line (Name)	Karyotype
HAP1 WT	Segmental chr. 15q gain	**4C 7**	n.s., 8 gain
dipHAP1 WT	Segmental chr. 15q gain	**4C 8**	n.s., 8 gain
4F 4	like HAP1 WT	**4C 11**	n.s., 8 gain
4F 13/ 1q gain parent	1q gain	**4C 18**	n.s., 8 gain
4F 16	1q gain, 8 gain	**4C 19**	n.s., 8 gain
4F 20	1q gain, 8 gain; presumably diploid	**2C 4**	1q gain, 8 gain
4F 23	1q gain	**2C 8**	1q gain, 8 gain, 21 gain

Under standard conditions, cell lines derived from the adapted 4F populations exhibited approximately 50% growth compared to HAP1 WT (Figure 9A, Supplemental Figure 5). Upon addition of reversine, cell line 4F 4, a cell line with a karyotype like HAP1 WT (Table 1) also grew very similarly to WT. Very notably however, all 4F cell lines with a gain in chromosome 1q rescued growth under reversine. 4F 14 and 4F 23, featuring only gains of chromosome 1q, showed a similar growth rescue with about 60% proliferation compared to standard. Cell lines 4F and the presumably diploid (Supplemental Figure 8) 4F 20, both exhibiting gains of chr. 1q and 8, grew the best.

While the 4C cell lines were not sequenced, according to the qPCR results (Supplemental Figure 4), they all gained chromosome 8. All 5 cell lines grew about 80% as well as WT under standard conditions (Figure 9B). Furthermore, they displayed robust growth under reversine, potentially implicating gain of chromosome 8 in reversine resistance. The gain of both chr. 1q and 8 in cell lines 2C 4 and 2C 8 conferred resistance to reversine, growing about 60 and 70% as well as under standard, respectively (Figure 9C).

The CFA data strongly suggests that the gain of an additional chromosome 1q is indicative of resistance to reversine in HAP1 cells. While gain of chromosome 8 could also be involved in resistance, the lack of sequencing data for cell line 4C prevents a definitive confirmation. The combined gain of chromosomes 1q and 8 could potentially increase resistance, but in any case, does not seem to negatively affect growth under reversine. In summary, this data affirms that the acquisition of single or multiple chromosomes, particularly chromosome 1q, can provide means for rescuing growth under reversine.

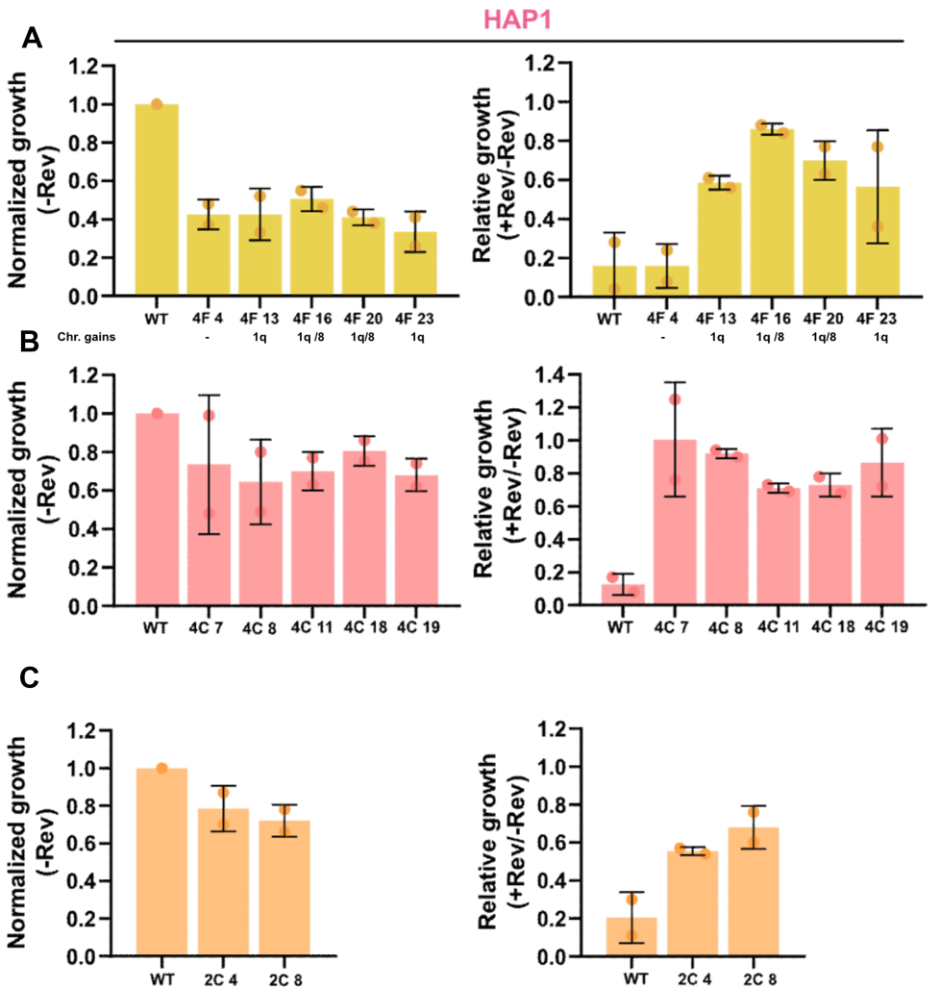

Figure 9: Growth measured by colony formation assay in HAP1 cells. (A, B, C) Growth measured by colony formation assay in 4F, 4C and 2C cell lines with (+Rev) and without (-Rev). Normalized growth was normalized to WT; relative growth was normalized to growth of the sample without reversine. n= indicated by points per bar graph.

3.2.3 Complex karyotypes in dipHAP1 cells complicate analysis of single chromosome gains

The same assay as for the HAP1 cell lines was then done for dipHAP1 cells. The sequencing results show that the karyotype of the diploid cell lines was much more complex with gains and losses of multiple chromosomes for each cell line (Table 2; Supplemental Figure 8). This complexity complicates data interpretation, as multiple explanations for any observed phenotypes are possible. Additional results of non-sequenced cell lines can be found in Supplemental Figure 4 and Supplemental Figure 5.

Most tested diploid cell lines exhibited losses of chromosome 13, 14 and/or chr. X, which were frequently observed in reversine adapted dipHAP1 cells (Adell & Klockner *et al*,

2023) and rescued growth under reversine. Cell lines with gains of chr. 1(q) or 8 increased reversine resistance, similar to HAP1 cells (Table 2; Figure 10).

Under standard conditions, certain cell lines, like #14 6, exhibited poorer growth than WT, both in absence and presence of reversine, despite the loss of chr. 13 and X. This growth disadvantage may be attributed to the loss of chr. 10q and gain of 10p. On the other hand, #14 21, with multiple gains and no losses, grew worse than WT under standard, but demonstrated high resistance to reversine, possibly due to chr. 1 gain. Despite lack of sequencing data, #11 17 likely harbors additional aneuploidies, but the identified gains of chr.1 and 8 seem to be important for reversine resistance. Intriguingly, despite losses in chr. 13, 14 and X, cell line #11 24 exhibited the poorest growth under standard and reversine among #11 cell lines (Figure 10C). Comparisons with #11 19 suggested that chr. 8 gains, additionally to chr. 13 and 14 losses, increases reversine resistance. Comparisons to #4 7 indicated that chr. 21 loss could contribute to this phenotype.

In cell lines #4 17 loss of chr. 7 may have increased reversine sensitivity, while our initial chromosome of interest, gain of chr. 5, showed varied phenotypes in #4 3 and #4 17 (Figure 10). For the #4 cell lines, a scratch assay (Supplemental Figure 2) was also conducted.

Table 2: Karyotype of indicated cell lines as identified by Illumnina sequencing or qPCR (n.s.= not sequenced).

Cell line (Name)	Karyotype	Cell line (Name)	Karyotype
HAP1 WT	Segmental chr. 15q gain	**dipHAP1 #14 6**	10q loss, 10p gain, 13 loss, X-loss
dipHAP1 WT	Segmental chr. 15q gain	**dipHAP1 #14 15**	5 gain, 9p gain, 13 loss, 14 loss, 21 loss, X-loss
dipHAP1 #4 1	n.s., 13q loss	**dipHAP1 #14 21**	1 gain, 3 gain, 7 gain, 11 gain, 20 gain
dipHAP1 #4 3	1q gain, 2 gain, 3 gain, 5 gain, 8 gain (2x), 20 gain, X-loss	**dipHAP1 #14 23**	1 gain, 13 loss, 14 loss, 21 gain, X-loss
dipHAP1 #4 7	13 loss, 14 loss, X-loss	**dipHAP1 #11 14**	3 gain, 8 gain, 13 loss, 14 loss, X-loss
dipHAP1 #4 14	n.s., 13q loss, 14q loss	**dipHAP1 #11 17**	n.s.; 1 gain, 8 gain
dipHAP1 #4 17	5 gain, 7 loss, 13 loss, 14 loss, X-loss	**dipHAP1 #11 19**	8 gain, 13 loss, 14 loss, X-loss
dipHAP1 #14 2	1 gain, 13 loss, 14 loss, X-loss	**dipHAP1 #11 24**	13 loss, 14 loss, 21 loss, X-loss

Taken together, interpreting the obtained CFA data for dipHAP1 cells is challenging due to their complex karyotypes. While losses of chr. 13, 14 and X generally increased reversine resistance, interactions between different aneuploidies can either enhance or diminish sensitivity to the drug, as exemplified by loss of chr. 21 in #11 24. However, consistent to the HAP1 growth data (Figure 9), chromosome 1 gain appeared to enhance reversine resistance in dipHAP1 cells and therefore was of peak interest for our further experiments.

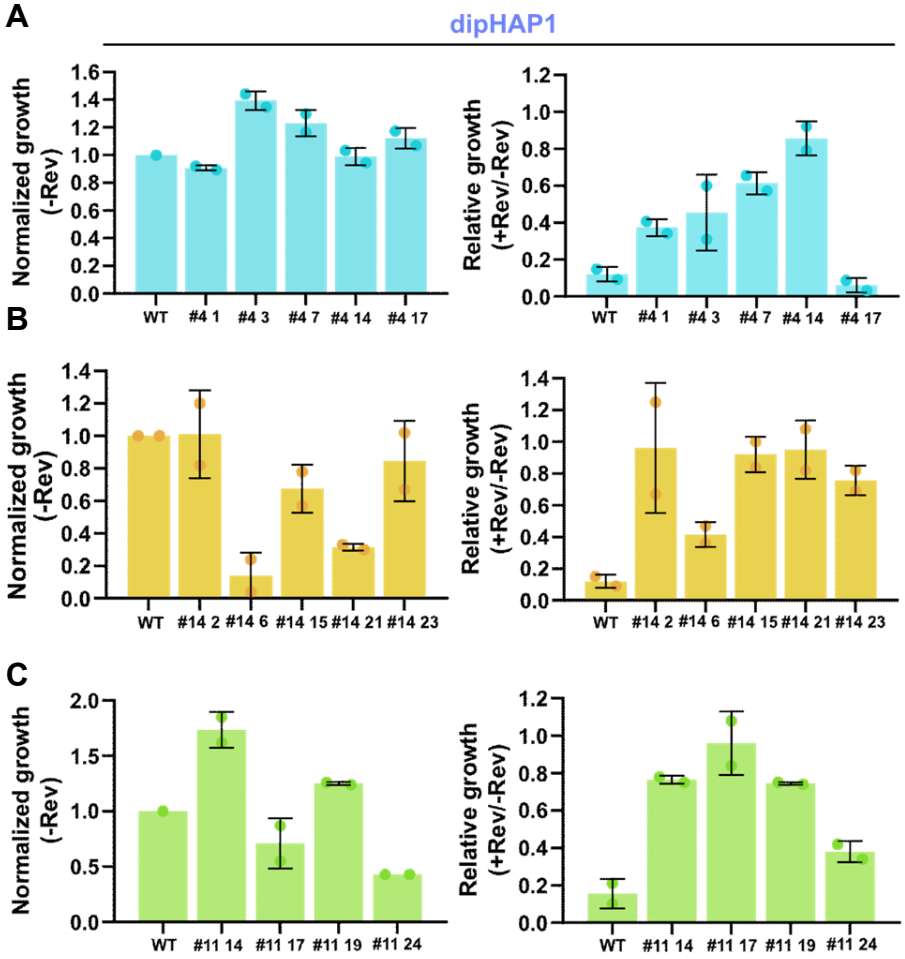

Figure 10: Growth measured by colony formation assay in dipHAP1 cells. (A, B, C) Growth measured by colony formation assay in #4, #14 and #11 cell lines with (+Rev) and without (-Rev). Normalized growth was normalized to WT; relative growth was normalized to growth of the sample without reversine. N= indicated by points per bar graph. Bars depict +/- SD.

3.3 CRISPR deletions of single chromosome (arm) gains

Having successfully established cell lines with gains in specific chromosomes, our next step was to further determine their role in reversine resistance. To achieve this, we wanted to delete specific gained chromosome arms, either fully or partially, to return to a WT copy

number. Then, we were able to compare the specific chromosome loss cell lines to the parental chromosome gain cell lines. For that, CRISPR guides were designed to cut at the centromere region of specific chromosomes (Table 7). As gain of the chromosome arm 1q confers resistance to reversine, we designed a sgRNA that targets the centromere to cut off the whole arm, as well as a second sgRNA guide to delete 1/3 genes of the chromosome arm starting from the telomere region. For chromosomes 5 and 8, we decided to target sgRNAs to both arms. After the CRISPR treatment and FACS single cell sort, cell lines were expanded clonally, and qPCR followed by Illumina sequencing was done to identify successful deletions. Next, we measured growth using colony formation assays. We then investigated if certain aneuploidies led to changes in mitotic timing and chromosome alignment defects, similar to loss of chromosome 13q or 6p as previously seen (Adell & Klockner *et al*, 2023).

3.3.1 Gain of chromosome 1q is sufficient for reversine resistance in HAP1 cells

Firstly, we sought to identify the role of chromosome 1q in reversine resistance in HAP1 cells. As gain of chromosome arm 1q was sufficient to rescue growth under reversine, a second guide was designed to cut off only the top 1/3 of the chromosome 1q (or tip) starting from the telomere region. As the genes *p31^{comet}* and *CDC16*, which we have already shown to increase reversine resistance, are involved with the SAC, this region was chosen to include the SAC-associated genes *PP2A-B56* (*PPP2R5A-B56*) and *PP1-15B* (*PPP1R15B*).

HAP1 4F 13 was chosen as the parental 1q gain cell line, which we used to engineer chromosome loses. Using the CRISPR approach, we were able to generate multiple 1q full loss cell lines, but none that just lost 1/3 of the arm (Figure 11A).

The findings from the CFA clearly demonstrate that the deletion of the gained chr. 1q and return to a euploid-like state increased sensitivity to reversine for all tested 1q del cell lines, while 1q gain conferred a robust resistance (Figure 11B, Supplemental Figure 9). This strongly implicates chromosome 1q gain in reversine resistance in HAP1 cells. Interestingly, in the absence of reversine, return to a WT-like karyotype by deletion of the gained chr. 1q did not rescue growth.

This observation suggests that the poor growth under standard exhibited by the parental 1q gain cell line, which is comparable to cell lines that lost the gained copy of chr. 1q, is not solely due to the presence of an additional chr. 1q.

Following our initial investigation into general cell proliferation, we set out to examine the intriguing question of whether gain of chromosome 1q had any influence on mitotic timing duration, both in presence and in absence of reversine (Figure 11D). Under standard conditions, the 1q deletion cell lines exhibited a slight elongation in mitotic timing compared to HAP1 WT, although the difference was not statistically significant. In contrast, the 1q gain parental cell lines, as well as the NC, displayed remarkable elongations of mitotic timing, increasing from ~26 min to ~30.5 and ~33 min, respectively. Reversine addition reinforced the role of 1q gain in mitotic timing. Notably, the 1q deletion cell lines and HAP1 WT cells saw a drastic decrease in their timing, while the 1q gain cell lines continued to significantly delay anaphase.

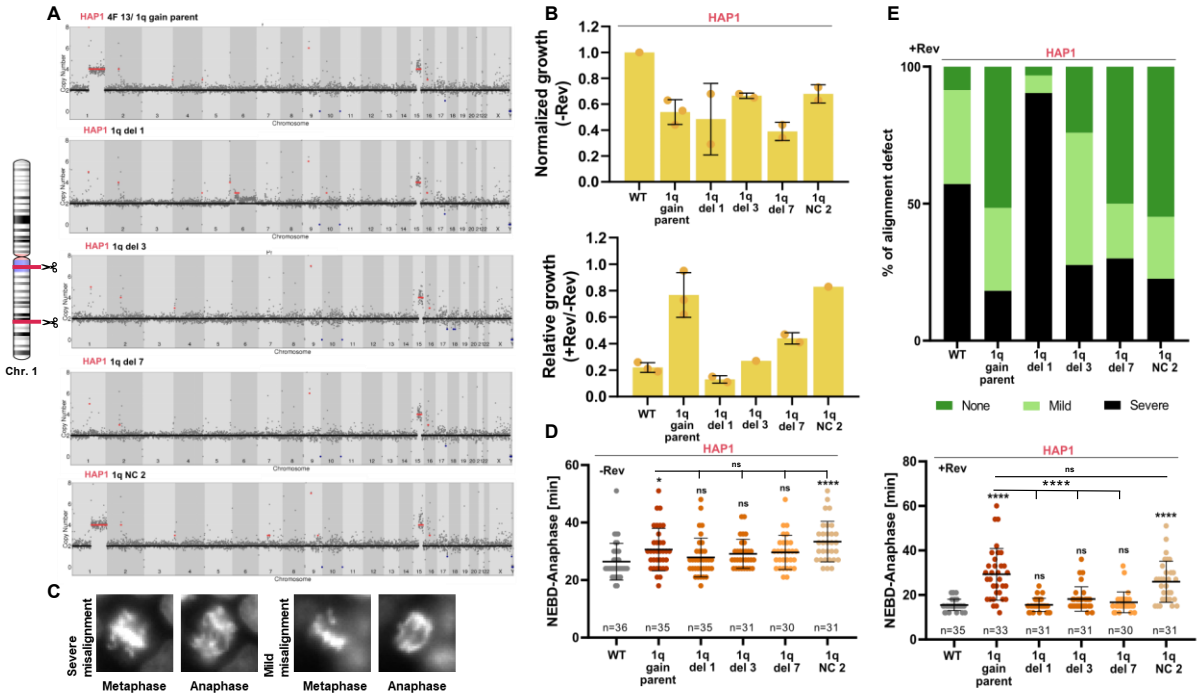

Figure 11: Gain of chromosme 1q increases reversine resistance in CFA and elongates mitotic timing in HAP1. (A) Copy number profiles for some of the HAP1 1q gain/del cell lines. (B) Growth measured by colony formation assay with (+Rev) and without (-Rev) reversine. Normalized growth was normalized to WT; relative growth was normalized to growth of the sample without reversine, n= indicated by points per bar graph. (C) Graphical depiction of mild and severe alignment defects. (D) Duration of NEBD-Anaphase in dCas9-VPR cell lines without reversine and with reversine. n= indicated below graphs. The bars represent the +/- SD value. P-values were obtained through ANOVA. Bars depict +/- SD (E) Quantification of alignment defects in HAP1 1q gain/del cell lines in percent.

Furthermore, we examined alignment defects by quantifying the chromosomes not aligned in the metaphase plate one image before anaphase occurred. One misaligned chromosome was classified as mild misalignment, more than one as a severe alignment defect (Figure 11C, E). The deletion of 1q gain was expected to increase alignment defects to a level comparable HAP1 WT. This assumption held true for cell line 1q del 1, in which approximately 90% of its mitotic events exhibited misaligned chromosomes, even higher than HAP1 WT. In contrast, the 1q gain cell lines improved chromosome alignment compared to WT (Figure 11E). The remaining two 1q deletion cell lines exhibited just marginally more alignment defects than the 1q gain cell lines. As flow cytometry data showed, a high percentage of the 1q del 1 cell line was likely diploid (Supplemental Figure 10). Given that diploids have twice as many chromosomes as haploid cells, it would make sense for diploids to exhibit more alignment defects. This notion in reinforced by comparison between the haploid HAP1 WT and diploid dipHAP1 WT alignment defects (Figure 11D, Figure 12D).

These results provide an insight in potential implication of chromosome 1q gain. In HAP1 cells, while not conferring general growth advantages in a CFA under standard conditions, chromosome 1q gain can confer resistance to reversine in a manner that elongates mitotic timing and potentially corrects alignment defects.

3.3.2 Gain of chromosome 1q is sufficient for reversine resistance in dipHAP1 cells

After uncovering the influence of chromosome 1q gain in reversine resistance in HAP1 cells, chromosome 1 gain was then investigated in dipHAP1 cells. As a parental 1 gain cell line, #14 21 was chosen and treated with CRISPR guides to delete chromosome 1q and 1q 1/3. In the diploids, we successfully engineered cell lines with both full and partial 1q loss and even obtained a cell line with chr. 1p loss, 1q NC 2, compared to the parental cell line (Figure 12A; Supplemental Figure 9).

Growth measured by CFA showed, that under standard conditions all cell lines, regardless of chromosome 1 gain or loss, grew comparably worse than WT (Figure 12B). The reversine CFA data for these cell lines displayed high standard deviations. This discrepancy was attributed to one of the experiments consistently yielding lower values, possibly due to a higher reversine concentration. However, when averaging the values, it

becomes evident that deletion of not only the entire arm 1q, but also deletion of the top 1/3 of genes increased reversine sensitivity. On the other hand, deletion of just the chr. 1p arm did not change resistance for 1q NC 2.

Looking at the mitotic timing data (Figure 12C) we see that compared to WT, all three tested cell lines exhibited extended timing in standard conditions, with the chr. 1 gain cell line displaying the most pronounced anaphase delay with ~40 min compared to ~21 min for the dipHAP1 WT. Excitingly, reversine addition revealed that deletion of both 1/3 and the full chr. arm 1q resulted in significantly faster timing than parental chr. 1 gain cell line, even if the multiple other aneuploidies these cell lines harbor likely impeded timing to return to WT levels. Next, we sought to compare the percentages of alignment defects to WT (Figure 12D). Impressively, the parental 1 gain cell line managed to rescue roughly

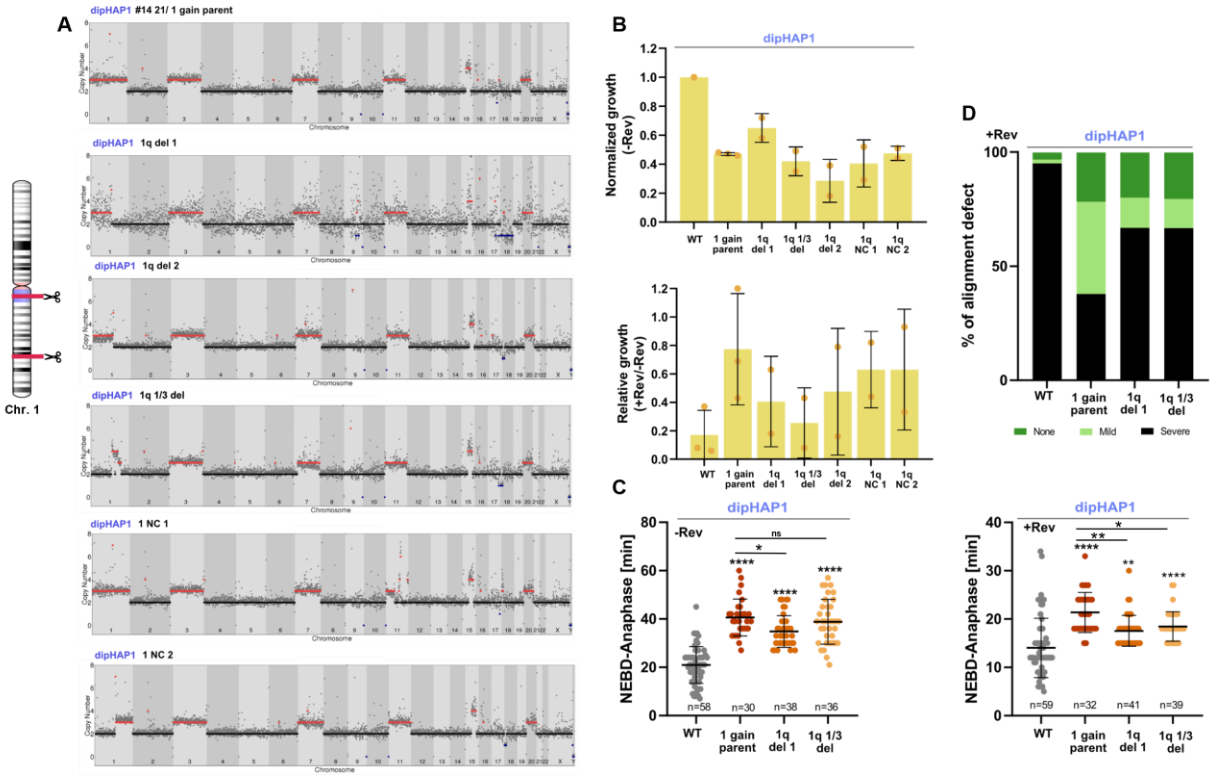

Figure 12: Gain of chromosme 1q and 1q 1/3 increases reversine resistance in CFA and elongates mitotic timing in dipHAP1. (A) Copy number profiles for some of the dipHAP1 1 gain/del cell lines. (B) Growth measured by colony formation assay with (+Rev) and without (-Rev) reversine. Normalized growth was normalized to WT; relative growth was normalized to growth of the sample without reversine, n= indicated by points per bar graph. (C) Duration of NEBD-Anaphase in dCas9-VPR cell lines without reversine and with reversine. n= indicated below graphs. The bars represent the +/- SD value. P-values were obtained through ANOVA. Bars depict +/- SD (D) Quantification of alignment defects in dipHAP1 1 gain/del cell lines in percent.

half of the severe alignment defects, while 1q del and 1q 1/3 del lost this improvement in chromosome alignment.

In light of these findings, it becomes evident that also in dipHAP1 cells chromosome 1q plays a pivotal role in reversine resistance. Additionally, the region of interest that is involved in conferring this resistance can be narrowed down to the 1q tip region containing 1/3 of the genes on this chromosome. In dipHAP1 cells the rescue was not as pronounced in HAP1 cells, likely due to the presence of multiple aneuploidies. We determined that in both HAP1 and dipHAP1 cells reversine resistance via gain of chromosome 1q is closely linked to an increase in mitotic duration and the improvement of chromosome alignment. These results lay a foundation for further research into specific chromosome regions and genes on chr. 1q that contribute to this phenotype.

3.3.3 Gain of chromosome 5 is not indicative of reversine resistance

After uncovering the role of chromosome 1q gain in reversine resistance, we conducted similar experiments in cell lines that gained chromosome 5 or 8.

After evaluating the first CFAs (Figure 10), we selected cell line #4 3 as a parental cell line with a gain in chromosome 5. Subsequently, we successfully generated cell lines harboring full chr. 5 deletions, 5p deletions and 5q deletions, along with negative controls (NC) where CRISPR treatment did not lead to chromosome loss (Figure 13A, Supplemental Figure 9).

Cell lines that lost either arm of chr. 5 or the entire chromosome grew better under standard condition than WT. However, upon the addition of reversine, while all cell lines showed a great rescue, it became evident that gain of full chromosome 5 or either arm did not considerably influence reversine resistance levels. The return to euploid chr. 5(p/q) levels did not substantially alter reversine resistance compared to the parental 5 gain cell line (Figure 13B; Supplemental Figure 6).

In this context, the rescue might be attributed to gains of other chromosomes, such as chr. 1, in this cell line.

To check whether chromosome 5 gain was implicated in increased invasiveness like seen in colon cancer cells (Vasudevan *et al*, 2020), we performed a scratch assay, which measures cell-migration capabilities by letting cells close a cell-free gap scratched into a

cellular monolayer under serum-starved conditions. A scratch was made into a monolayer of different dipHAP1 cell lines and pictures were taken immediately following the scratch and after 48. The normalized closing rate was calculated by dividing the distance between the edged of the scratch immediately after the scratch by the distance after 48h and normalizing to WT. The scratch assay showed that gain of chromosome 5 does not majorly impact the closing rate compared to WT (Figure 13C). CFA and scratch assay data for more cell lines can be found in Supplemental Figure 6.

In summary, this data suggests, that chromosome 5 is not indicated in reversine resistance for dipHAP1 cells and it does not lead to increased gap-closure in this cell type.

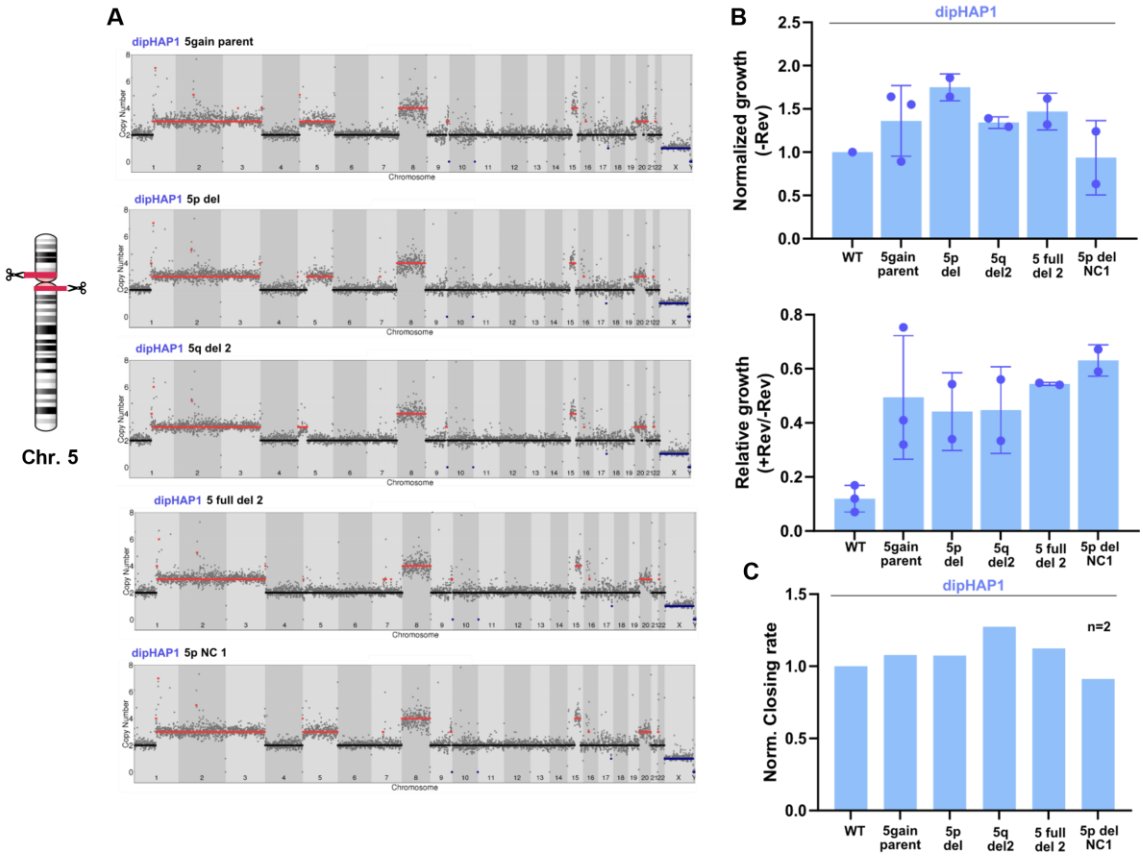

Figure 13: Growth measured by CFA and scratch assay in chr. 5 gain/deletion cell lines. (A) Copy number profiles for some of the dipHAP1 5gain/del cell lines. (B) Growth measured by colony formation assay with (+Rev) and without (-Rev) reversine. Normalized growth was normalized to WT; relative growth was normalized to growth of the sample without reversine, n= indicated by points per bar graph. (C) Scratch assay results for 5gain/del cell lines. Bars depict +/- SD.

3.3.4 Gain of chromosome 8 might slightly increase reversine resistance in dipHAP1

To investigate effects of chromosome 8 gain in dipHAP1 cells, we CRISPR-treated dipHAP1 #11 14 as our 8 gain-parental cell line. We generated cell lines that fully lost chromosome 8 once (8 full del 1) or twice (8 full del 2), which only had one copy of chr. 8 left, and negative controls NC. We were also able to obtain a cell line with loss of chr. 8q (Figure 14A; Supplemental Figure 9).

In absence of reversine, only cell line 8 full del 2 grew considerably worse than WT (Figure 14B). This cell line also demonstrated the weakest reversine resistance among these engineered cell lines, although the reliability of this value is compromised by a high standard deviation. The 8q deletion displayed better rescue than 8 full del 1, suggesting a potential role for chr. arm 8p in reversine resistance. The parental 8 gain cell line showed only a marginal growth advantage under reversine compared to the chr. 8 full deletion 1 and the negative control 8p NC1. The chr. 8 monosomy proved sensitive to reversine but gain of 8 alone may not suffice for reversine resistance in dipHAP1 cells.

Looking at the scratch assay results (Figure 14C), the chr. 8 monosomic cell line reduced the cell migration capacity compared to the 8 gain parental cell line, nearly reaching WT levels. The return to euploid chr. 8 levels in cell line 8 full del slightly decreased the closing rate compared to 8 gain parent. The 8q del cell line displayed remarkable efficiency in closing the gap. However, in Supplemental Figure 9, the presumably tetraploid cell line 8q del 4n, with 8q loss, exhibited a closing rate more comparable to the chr. 8 full del cell line. This rather suggests that the migration capacity of the 8q del cell line may not be solely dependent on the gain of chr. 8p, but rather on different genomic changes.

Together, this data indicates that monosomy of chromosome 8 is generally detrimental for proliferation, cell migration and increases sensitivity to reversine. Additionally, gain of chromosome 8 could potentially have a slight impact on reversine resistance in dipHAP1 cells. Investigating the gain of chromosome 8 in the haploid cell lines could shed further light on its potential in rescuing reversine resistance.

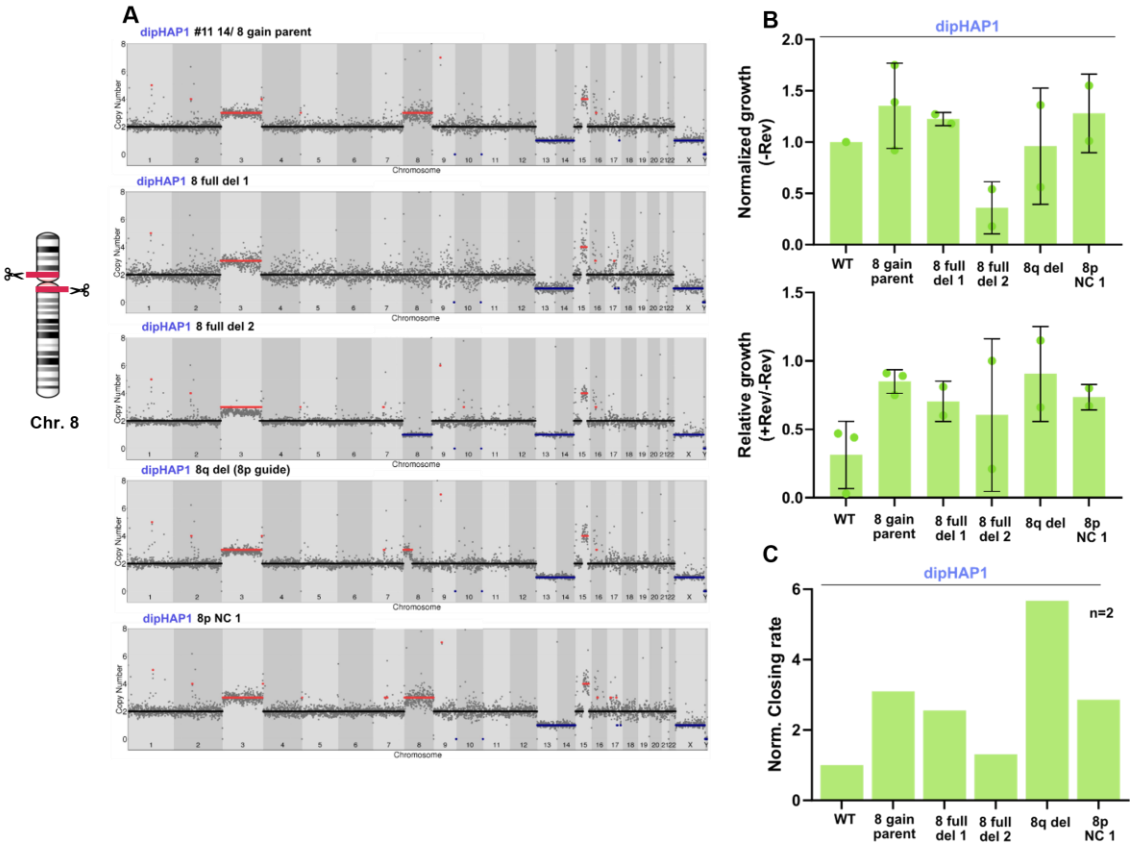

Figure 14: Growth measured by CFA and scratch assay in chr. 8 gain/deletion cell lines. (A) Copy number profiles for some of the dipHAP1 8gain/del cell lines. (B) Growth measured by colony formation assay with (+Rev) and without (-Rev) reversine. Normalized growth was normalized to WT; relative growth was normalized to growth of the sample without reversine, n= indicated by points per bar graph. (C) Scratch assay results for 8gain/del cell lines. Bars depict +/- SD.

4 Discussion

During the course of this thesis, I implemented a CRISPR-activation system in dipHAP1 cell lines, through which I could study overexpression of genes previously found to confer resistance to the drug reversine if reduced by one copy number. Using this approach, I was able to further determine, that genes *p31^{comet}* and *CDC16* are involved in modulating the timing of mitosis and through this can increase resistance to reversine.

Additionally, I investigated the role of frequent chromosome gains acquired in the adaptation to reversine. To identify the role of those gains in resistance, I deleted one copy of the gained chromosomes in adapted cell lines via CRISPR/Cas9 to revert the copy number back to euploid levels and subsequently analyzed the phenotype of the adapted cell lines with and without the frequent chromosome gains.

4.1 Overexpression of genes *p31^{comet}* and *CDC16* via CRISPRa strengthened their role in reversine resistance

As previously established, engineered monosomies of chromosome 13q and 6p confer resistance to the drug reversine by extending mitotic timing and improving alignment of chromosomes (Figure 2B, C; Adell & Klockner *et al*, 2023). Genes that were identified as drivers of the resistance are *CDC16* on chr. 13q and *p31^{comet}* on chr. 6p. Based on these findings, I wanted to determine whether *CDC16* and *p31^{comet}* were solely responsible for the phenotype or if other genes on the chromosome contribute to the observed phenotype. To investigate this, I established the CRISPRa system in dipHAP1 cell lines. For the overexpression experiments I used cell lines for which western blotting confirmed the decreased *CDC16* or *p31^{comet}* levels in dipHAP1 cell lines monosomic for 13q, 6p or in a *CDC16* heterozygous knockout cell line. Using lentiviral transduction, the above mentioned engineered dipHAP1 cell lines as well as a dipHAP1 WT cell line were engineered to express a dCas9-VPR fusion protein, which induces overexpression of targeted genomic loci depending on the specificity of the used sgRNAs. Indeed, after transfection with guides for *CDC16*, *p31^{comet}* and *TTN* as an overexpression control, we saw an increase in RNA expression of these genes in a dCas9-VPR WT background via RTqPCR. However, the confirmation of the overexpression in the deletion cell lines was not as successful, with RNA levels partially even decreasing. Looking at the Ct values for

the reference gene *GAPDH* (Table 11) we see that the values are not consistent. As we selected cells for at least 5 days using G418 to obtain enough cells for RTqPCR, it could be possible that the extended exposure to this antibiotic led to changes in expression of some genes. Cultivation for longer periods of time also leads to loss of the resistance plasmid over time as it is not replicated, leading cells to express less of the sgRNA. These challenges in the overexpression system could influence the obtained RTqPCR levels of all analyzed genes. To optimize RTqPCR results switching to a different reference gene than *GAPDH* may lead to more consistent results. Testing of different sgRNA guide plasmids and optimizing the transfection efficiency could shorten the selection time needed in G418. Alternatively, induction of sgRNA delivery, like induction via doxycycline could be useful to directly compare the same cell lines before and after induction.

However, measurements of the mitotic timing revealed that while the addition of sgRNAs targeting *CDC16* or *p31^{comet}* did not change timing in dCas9-VPR-WT cells, it significantly decreased time spent in mitosis in the dCas9-VPR-13q, dCas9-VPR-6p and dCas9-VPR-CDC16+/- cell lines in standard conditions. Knowing that both CDC16 and p31^{comet} are promoters of anaphase, their increased presence would be expected to lead to a shorter mitotic duration, which is what I could observe. Notably, a delay in mitotic timing by several minutes was not only observed in absence, but also in presence of reversine, pointing even more strongly toward the role of *CDC16* or *p31^{comet}* in modulating mitotic timing. Under standard conditions, the mitotic timing of the 13q and 6p loss cell lines was not decreased to that of the dCas9-VPR-WT cell line, while in dCas9-VPR-CDC16+/-, mitotic duration after CDC16 guide addition was very comparable to WT. One explanation could be, that other genes on chromosomes 13q and 6p influence mitotic timing. Also, the different acquired aneuploidies could be causing some of the delay.

These results suggest, that despite the RTqPCR results, CRISPRa induced overexpression was indeed successful in in live-cell experiments and resulted in changes in mitotic timing. In dCas9-VPR-WT, higher expression levels of *p31^{comet}* and *CDC16* did not result in a change in mitotic duration. Both *p31^{comet}* and *CDC16* are not acting alone but in cooperation with other protein(s). Therefore, overexpression of just these genes alone and not also their partners could result in stochiometric imbalances and excess of overexpressed genes, possibly negatively affecting with different pathways. However, for

CDC16 and *p31^{comet}*, this does not seem to influence their function in regulating mitotic duration as exemplified by the sgRNA addition in WT. However, even if RNA levels are increased, it does not necessarily mean protein levels are similarly increased (Gry *et al*, 2009). To check this, testing changes in protein levels via western blot would be necessary to confirm the overexpression.

Taken together, the anticipated overexpression of *CDC16* and *p31^{comet}* RNA levels was not conclusively confirmed, but observed phenotypic changes in mitotic timing underscored the effectiveness of the CRISPRa system. Through this research I was able to strengthen the pivotal role of both *CDC16* and *p31^{comet}* in regulating mitotic timing and their involvement in reversine resistance. The findings contribute to our understanding of the involvement of these genes in conferring reversine resistance.

4.2 Chromosome gains

4.2.1 Analysis of specific chromosome gains is complicated in cell lines with complex karyotypes

Chromosomes 8(q) and 1(q) are frequently gained in different cancers (Taylor *et al*, 2018) as well as in cells adapted to reversine (Adell & Klockner *et al*, 2023). Similarly, chromosome 5 gain is seen in cancer (Knouse *et al*, 2017) and, to a lesser extent, obtained upon reversine adaptation. In the adapted cell lines #4, #14 and #11 that we choose, gains and losses of a number of different chromosomes are common. Especially losses of chromosomes 13 and 14 were often observed and in agreement with previous findings (Adell & Klockner *et al*, 2023) increased reversine resistance. For other aneuploidies, the karyotypes were too complex to attribute a single chromosome loss or gain event to reversine resistance. As the reversine adaptation approach led to dipHAP1 cells acquiring multiple aneuploidies that eventually converged upon an optimal karyotype, different gains and losses act together to enable the best rescue. Additionally, for all adapted cell lines it has to be kept in mind, that mutations or other alterations like epigenetic changes were not checked for any of these cell lines.

4.2.2 Gain of chromosome 5 is not implicated in migration and reversine resistance in dipHAP1 cells

Gain of chromosome 5 was previously implicated in increasing the migrative capacities in HCT116 cells (Vasudevan *et al*, 2020). Using the generated CRISPR deletion cell lines in which we reverted the gain of chromosome 5 back to euploid levels, we could show that reversion of neither 5q, 5p or full chromosome 5 changed growth under reversine or in standard conditions. The scratch assay data also did not indicate a significant change in migratory capacities of cell lines with or without the gain of chromosome 5. Collectively, gain of chromosome 5 in dipHAP1 cells upon reversine adaptation does not confer an advantage that can be measured by the assays we choose.

4.2.3 Unclear role of chromosome 8 in reversine resistance

In the HAP1 4C cell lines that had chr. 8 gains, we saw that this gain indeed led to an extremely good rescue in reversine. Not having sequenced those cells, we cannot exclude that any additional genomic changes influenced this resistance. In dipHAP1 cells, using CRISPR guides, we could delete the gained chr. 8q or full chr. 8 and even obtained a chr. 8 monosomic cell line. In the absence of reversine, chr. 8 monosomy decreased proliferation compared to WT. Gain of chromosome 8 slightly improved migration in a scratch assay compared to a cell line that lost the gained chromosome 8, which in turn had better gap-closing capabilities than the monosomy. This might indicate chromosome 8 gain in increased migration capacities in dipHAP1 cells, while chr. 8 monosomy is detrimental for proliferation, cell migration and reversine resistance. To obtain a clearer picture, repeating the CRISPR deletion approach in 4C 8-gain HAP1 cells would be of interest.

4.2.4 Chromosome 1q gain is sufficient to rescue growth in reversine

Chromosome 1 gain, especially chr. arm 1q is very common in different cancers (Taylor *et al*, 2018) and its gain was also common during the (dip)HAP1 reversine adaptation experiments. In HAP1 1q gain cells (4F), colony formation assays revealed that cell lines with 1q gain had a remarkable rescue under reversine. Intriguingly, a HAP1 4F cell line without 1q gain showed no rescue of growth compared to WT cells. In standard conditions, all 4F cell lines grew about 30-50% as WT cells, independent of having 1q gain. This very

strongly implicated, that gain of chr. arm 1q can rescue growth under reversine, but, at least in HAP1 cells, likely does not contribute to a general growth advantage. DipHAP1 chr. 1 gain cells (#14) displayed a much more complex karyotype which made identifying the individual role of whole chromosome 1 gain very difficult. All the #14 cell lines that had a gain of 1q in addition to other aneuploidies, had a great reversine rescue. This points into the direction that chr. 1 gain also plays a role in conferring reversine resistance in dipHAP1 cells.

To confirm these results, we deleted both full chr. 1q arm, as well as only the tip of chromosome 1q starting from the telomere, containing 1/3 of the genes, to narrow down the region of the chromosome that confers this observed resistance. For HAP1 cells, we just obtained cell lines with loss of whole 1q arm. Growth measured by CFA showed, that full 1q deletion decreased reversine resistance compared to the 1q gain parent cell line and for some of them even brought resistance down to WT levels. In addition to CFAs, we measured mitotic timing to check whether the resistance to reversine was achieved through a change in mitotic timing. In standard conditions, timing for both the 1q gain parental cell line (4F 13) and a 1q negative control, with the 1q gain, was significantly longer than WT timing. The duration of mitosis for 1q deletion cell lines, however, was very similar to HAP1 WT. Addition of reversine revealed, that cell lines with 1q gain had a long mitotic delay compared to deletion cell lines. This strongly suggest a role for 1q gain in extending mitotic timing. Counting the percentage of alignment defects showed, that while one of the 1q del cell lines, that was also partially diploid, increased the number of alignment defects drastically, the other ones were very similar to 1q gain cell lines, leading to the assumption that parental 1q gain cell line may had mechanisms other than 1q gain to help with alignment improvements.

In dipHAP1 cells, using CRISPR we obtained cell lines with 1q and 1q 1/3 loss and even a cell lines with loss of 1p. Like in HAP1 cells, deletion of chr. arm 1q decreased reversine rescue, while loss of 1p did not change resistance levels. Interestingly, deletion of 1/3 of genes on chromosome arm 1q also decreased resistance. Mitotic timing also showed that deletion of 1q and 1q 1/3 significantly decreased mitotic timing compared to the 1 gain parent both under reversine and without. The mitotic duration was still increased compared to WT, likely due to some of the multiple obtained chromosome gains. In

contrast to HAP1 cells, deletion of 1q or 1q 1/3 increased the percentage of cells with severe alignment defects. Therefore, genes in the 1q 1/3 region could be important in regulating chromosome alignment.

Collectively, we determined that gain of chromosome arm 1q both in HAP1 and dipHAP1 cells helps rescue growth under reversine by elongating mitotic timing and, at least in dipHAP1 cells, by benefiting chromosome alignment before anaphase. The region of interest seems to be the tip region containing 1/3 genes of chromosome arm 1q, as its phenotype is extremely similar to the loss of whole chr. 1q.

When looking at genes that are involved in the spindle assembly checkpoint and therefore have control in timing mitosis, possible candidate genes in this region are *PPP2R5A-B56* (or *PP2A-B56*) and *PPP1R15B* (or *PP1-15B* here, interacts with PP1). Interestingly, both proteins favor exit of mitosis as opposed to aiding the SAC and increasing mitotic timing making their role in reversine resistance unclear. PP2A-B56 counteracts MPS1 signaling at the kinetochore through the dephosphorylation of KNL1, while PP1 binds to sites on KNL1 that were dephosphorylated by PP2A-B56 and helps switch of the SAC (McAinsh & Kops, 2023; Espert *et al*, 2014). However, it has been suggested (Gelens & Saurin, 2018), that both PP2A-B56 and MPS1 together help in driving binding and releasing of mitotic checkpoint components, possibly enhancing SAC signaling. To further investigate the role of these phosphatases in reversine resistance, the analysis of the protein levels in cell lines with and without the 1q gain will be necessary. If protein levels are indeed reflecting the copy number, engineering knockout cell lines with the heterozygous loss of *PP2A-B56* or *PP1-15B* in chromosome 1q gain cell lines and analyzing them with colony formation assays and live cell imaging will shed light on their role in reversine resistance. Because there are still a lot of genes in the 1q 1/3 region, narrowing down more candidate drivers will be difficult. Smaller deletions of this region of interest by introducing multiple CRISPR-cut sites could narrow down the region further and point towards genes of interest.

Altogether, we found that, while gained in adapted cell lines, gain of chromosome 5 does not seem to be implicated in either reversine resistance or offering general growth advantages in dipHAP1 cells. Chromosome 8 gain might have a role in reversine resistance, but further experiments are needed to explore its role in dipHAP1 cells.

Monosomy of chr. 8 in dipHAP1 cells however decreases proliferation and reversine resistance. In HAP1 cells, deletion of 8 gain could help strengthening the role for chr 8 gain in reversine resistance. Studying those haploid cell lines aid in this endeavor.

We were however able to positively identify gain of chromosome 1q, especially the tip region containing 1/3 of genes on this arm, in being pivotal for reversine resistance. Both rescuing growth under reversine and elongating mitotic timing in HAP1 and dipHAP1 cells, genes on this chromosome that confer resistance are likely involved in mitosis like *p31^{comet}* or *CDC16*. It will be interesting to further investigate the role of two candidate genes *PPP2A-B56* and *PP1-15B* as potential drivers of the 1q gain in HAP1 and dipHAP1 cells.

4.3 Significance and outlook

In this thesis, the influence of cellular adaptation via acquisition of different aneuploidies and their role in reversine resistance was explored. Through overexpression of the genes *p31^{comet}* and *CDC16* in cell line heterozygous for these genes, their role in reversine resistance was further investigated. Furthermore, we examined the involvement of specific chromosome gains. Particularly chromosome 1q was implicated in conferring resistance to the drug reversine and altering mitotic timing. The chromosomal region most important for the resistance, in which genes including *PPP2A-B56* and *PP1-15B* lay, was identified. Assays to explore the role of those genes and narrowing down the resistance conferring region on chr. 1q are important for the potential identification of genes implicated in the resistance. Through this research we established a lot of different cell lines with a multitude of aneuploidies, offering potential avenues for further experiments to elucidate the impact of more chromosome gains or losses on both cellular growth and drug resistance. Specific aneuploidies, including gains of chromosome 1 or loss of chromosome 13, are frequently observed in some cancers (Knouse *et al*, 2017; Micale *et al*, 1994) and can be beneficial for cancer growth. Unraveling how and why different aneuploidies emerge can be useful for understanding how tumors evolve. Identifying driver aneuploidies and finding ways to target them specifically can hold future treatment possibilities. Additionally, pinpointing individual genes that can confer a growth advantage sufficient to offset the negative consequences of aneuploidy holds promise for therapeutic strategies specifically designed to just target these genes.

5 Sources

Adell MAY, Klockner TC, Höfler R, Wallner L, Schmid J, Markovic A, Martyniak A & Campbell CS (2023) Adaptation to spindle assembly checkpoint inhibition through the selection of specific aneuploidies. *Genes Dev* 37: 171–190

Anjur-Dietrich MI, Kelleher CP & Needleman DJ (2021) Mechanical Mechanisms of Chromosome Segregation. *Cells* 10: 465

Bae S, Park J & Kim J-S (2014) Cas-OFFinder: a fast and versatile algorithm that searches for potential off-target sites of Cas9 RNA-guided endonucleases. *Bioinformatics* 30: 1473–1475

Ben-David U & Amon A (2020) Context is everything: aneuploidy in cancer. *Nat Rev Genet* 21: 44–62

Cai Y, Crowther J, Pastor T, Abbasi Asbagh L, Baietti MF, De Troyer M, Vazquez I, Talebi A, Renzi F, Dehairs J, *et al* (2016) Loss of Chromosome 8p Governs Tumor Progression and Drug Response by Altering Lipid Metabolism. *Cancer Cell* 29: 751–766

Carmena M, Wheelock M, Funabiki H & Earnshaw WC (2012) The chromosomal passenger complex (CPC): from easy rider to the godfather of mitosis. *Nat Rev Mol Cell Biol* 13: 789–803

Chavez A, Scheiman J, Vora S, Pruitt BW, Tuttle M, P R Iyer E, Lin S, Kiani S, Guzman CD, Wiegand DJ, *et al* (2015) Highly efficient Cas9-mediated transcriptional programming. *Nat Methods* 12: 326–328

Cheeseman IM (2014) The Kinetochore. *Cold Spring Harbor Perspectives in Biology* 6: a015826–a015826

Clarke MN, Marsoner T, Adell MAY, Ravichandran MC & Campbell CS (2023) Adaptation to high rates of chromosomal instability and aneuploidy through multiple pathways in budding yeast. *The EMBO Journal* 42: e111500

Concordet J-P & Haeussler M (2018) CRISPOR: intuitive guide selection for CRISPR/Cas9 genome editing experiments and screens. *Nucleic Acids Research* 46: W242–W245

Davoli T, Xu AW, Mengwasser KE, Sack LM, Yoon JC, Park PJ & Elledge SJ (2013) Cumulative Haploinsufficiency and Triplosensitivity Drive Aneuploidy Patterns and Shape the Cancer Genome. *Cell* 155: 948–962

DeLuca JG, Gall WE, Ciferri C, Cimini D, Musacchio A & Salmon ED (2006) Kinetochore Microtubule Dynamics and Attachment Stability Are Regulated by Hec1. *Cell* 127: 969–982

Espert A, Uluocak P, Bastos RN, Mangat D, Graab P & Gruneberg U (2014) PP2A-B56 opposes Mps1 phosphorylation of Knl1 and thereby promotes spindle assembly checkpoint silencing. *Journal of Cell Biology* 206: 833–842

Ganem NJ, Godinho SA & Pellman D (2009) A mechanism linking extra centrosomes to chromosomal instability. *Nature* 460: 278–282

Gelens L & Saurin AT (2018) Exploring the Function of Dynamic Phosphorylation-Dephosphorylation Cycles. *Developmental Cell* 44: 659–663

Girish V, Lakhani AA, Thompson SL, Scaduto CM, Brown LM, Hagenson RA, Sausville EL, Mendelson BE, Kandikuppa PK, Lukow DA, *et al* (2023) Oncogene-like addiction to aneuploidy in human cancers. *Science* 381: eadg4521

Gry M, Rimini R, Strömberg S, Asplund A, Pontén F, Uhlén M & Nilsson P (2009) Correlations between RNA and protein expression profiles in 23 human cell lines. *BMC Genomics* 10: 365

Hassold T & Hunt P (2001) To err (meiotically) is human: the genesis of human aneuploidy. *Nat Rev Genet* 2: 280–291

Holland AJ & Cleveland DW (2012) Losing balance: the origin and impact of aneuploidy in cancer: 'Exploring aneuploidy: the significance of chromosomal imbalance' review series. *EMBO Reports* 13: 501–514

Ippolito MR, Martis V, Martin S, Tijhuis AE, Hong C, Wardenaar R, Dumont M, Zerbib J, Spierings DCJ, Fachinetti D, *et al* (2021) Gene copy-number changes and chromosomal instability induced by aneuploidy confer resistance to chemotherapy. *Developmental Cell* 56: 2440-2454.e6

Kahlem P, Sultan M, Herwig R, Steinfath M, Balzereit D, Eppens B, Saran NG, Pletcher MT, South ST, Stetten G, *et al* (2004) Transcript Level Alterations Reflect Gene Dosage Effects Across Multiple Tissues in a Mouse Model of Down Syndrome. *Genome Res* 14: 1258–1267

Kent WJ, Sugnet CW, Furey TS, Roskin KM, Pringle TH, Zahler AM & Haussler AD (2002) The Human Genome Browser at UCSC. *Genome Res* 12: 996–1006

Knouse KA, Davoli T, Elledge SJ & Amon A (2017) Aneuploidy in Cancer: Seq-ing Answers to Old Questions. *Annu Rev Cancer Biol* 1: 335–354

Kojima S & Cimini D (2019) Aneuploidy and gene expression: is there dosage compensation? *Epigenomics* 11: 1827–1837

Krenn V & Musacchio A (2015) The Aurora B Kinase in Chromosome Bi-Orientation and Spindle Checkpoint Signaling. *Front Oncol* 5

Labun K, Montague TG, Krause M, Torres Cleuren YN, Tjeldnes H & Valen E (2019) CHOPCHOP v3: expanding the CRISPR web toolbox beyond genome editing. *Nucleic Acids Research* 47: W171–W174

Lara-Gonzalez P, Pines J & Desai A (2021) Spindle assembly checkpoint activation and silencing at kinetochores. *Seminars in Cell & Developmental Biology* 117: 86–98

Lee AJX, Endesfelder D, Rowan AJ, Walther A, Birkbak NJ, Futreal PA, Downward J, Szallasi Z, Tomlinson IPM, Howell M, *et al* (2011) Chromosomal Instability Confers Intrinsic Multidrug Resistance. *Cancer Research* 71: 1858–1870

Li M, Fang X, Baker DJ, Guo L, Gao X, Wei Z, Han S, Van Deursen JM & Zhang P (2010) The ATM–p53 pathway suppresses aneuploidy-induced tumorigenesis. *Proc Natl Acad Sci USA* 107: 14188–14193

Lukow DA, Sausville EL, Suri P, Chunduri NK, Wieland A, Leu J, Smith JC, Girish V, Kumar AA, Kendall J, *et al* (2021) Chromosomal instability accelerates the evolution of resistance to anti-cancer therapies. *Developmental Cell* 56: 2427-2439.e4

Maiato H & Silva S (2023) Double-checking chromosome segregation. *Journal of Cell Biology* 222: e202301106

McAinsh AD & Kops GJPL (2023) Principles and dynamics of spindle assembly checkpoint signalling. *Nat Rev Mol Cell Biol* 24: 543–559

Micale MA, Visscher DW, Gulino SE & Wolman SR (1994) Chromosomal aneuploidy in proliferative breast disease. *Human Pathology* 25: 29–35

Musacchio A (2015) The Molecular Biology of Spindle Assembly Checkpoint Signaling Dynamics. *Current Biology* 25: R1002–R1018

Nasmyth K & Haering CH (2009) Cohesin: Its Roles and Mechanisms. *Annu Rev Genet* 43: 525–558

Nicholson JM & Cimini D (2013) Cancer Karyotypes: Survival of the Fittest. *Front Oncol* 3

Passerini V, Ozeri-Galai E, De Pagter MS, Donnelly N, Schmalbrock S, Kloosterman WP, Kerem B & Storchová Z (2016) The presence of extra chromosomes leads to genomic instability. *Nat Commun* 7: 10754

Perez-Pinera P, Kocak DD, Vockley CM, Adler AF, Kabadi AM, Polstein LR, Thakore PI, Glass KA, Ousterout DG, Leong KW, *et al* (2013) RNA-guided gene activation by CRISPR-Cas9–based transcription factors. *Nat Methods* 10: 973–976

Ravichandran MC, Fink S, Clarke MN, Hofer FC & Campbell CS (2018) Genetic interactions between specific chromosome copy number alterations dictate complex aneuploidy patterns. *Genes Dev* 32: 1485–1498

Sansregret L, Patterson JO, Dewhurst S, López-García C, Koch A, McGranahan N, Chao WCH, Barry DJ, Rowan A, Instrell R, *et al* (2017) APC/C Dysfunction Limits Excessive Cancer Chromosomal Instability. *Cancer Discovery* 7: 218–233

Sansregret L, Vanhaesebroeck B & Swanton C (2018) Determinants and clinical implications of chromosomal instability in cancer. *Nat Rev Clin Oncol* 15: 139–150

Santaguida S, Richardson A, Iyer DR, M'Saad O, Zasadil L, Knouse KA, Wong YL, Rhind N, Desai A & Amon A (2017) Chromosome Mis-segregation Generates Cell-Cycle-Arrested Cells with Complex Karyotypes that Are Eliminated by the Immune System. *Developmental Cell* 41: 638-651.e5

Schmidt H, Zhang M, Mourelatos H, Sánchez-Rivera FJ, Lowe SW, Ventura A, Leslie CS & Pritykin Y (2022) Genome-wide CRISPR guide RNA design and specificity analysis with GuideScan2 Genomics

Schukken KM & Sheltzer JM (2022) Extensive protein dosage compensation in aneuploid human cancers. *Genome Res* 32: 1254–1270

Sheltzer JM, Blank HM, Pfau SJ, Tange Y, George BM, Humpton TJ, Brito IL, Hiraoka Y, Niwa O & Amon A (2011) Aneuploidy Drives Genomic Instability in Yeast. *Science* 333: 1026–1030

Shoshani O, Bakker B, De Haan L, Tijhuis AE, Wang Y, Kim DH, Maldonado M, Demarest MA, Artates J, Zhengyu O, *et al* (2021) Transient genomic instability drives tumorigenesis through accelerated clonal evolution. *Genes Dev* 35: 1093–1108

Silk AD, Zasadil LM, Holland AJ, Vitre B, Cleveland DW & Weaver BA (2013) Chromosome missegregation rate predicts whether aneuploidy will promote or suppress tumors. *Proc Natl Acad Sci USA* 110

Su XA, Ma D, Parsons JV, Replogle JM, Amatruda JF, Whittaker CA, Stegmaier K & Amon A (2021) *RAD21* is a driver of chromosome 8 gain in Ewing sarcoma to mitigate replication stress. *Genes Dev* 35: 556–572

Tanaka TU (2005) Chromosome bi-orientation on the mitotic spindle. *Phil Trans R Soc B* 360: 581–589

Taylor AM, Shih J, Ha G, Gao GF, Zhang X, Berger AC, Schumacher SE, Wang C, Hu H, Liu J, *et al* (2018) Genomic and Functional Approaches to Understanding Cancer Aneuploidy. *Cancer Cell* 33: 676-689.e3

Thompson SL, Bakhoum SF & Compton DA (2010) Mechanisms of Chromosomal Instability. *Current Biology* 20: R285–R295

Thorburn RR, Gonzalez C, Brar GA, Christen S, Carlile TM, Ingolia NT, Sauer U, Weissman JS & Amon A (2013) Aneuploid yeast strains exhibit defects in cell growth and passage through START. *MBoC* 24: 1274–1289

Tijhuis AE, Johnson SC & McClelland SE (2019) The emerging links between chromosomal instability (CIN), metastasis, inflammation and tumour immunity. *Mol Cytogenet* 12: 17

Torres EM, Sokolsky T, Tucker CM, Chan LY, Boselli M, Dunham MJ & Amon A (2007) Effects of Aneuploidy on Cellular Physiology and Cell Division in Haploid Yeast. *Science* 317: 916–924

Vasudevan A, Baruah PS, Smith JC, Wang Z, Sayles NM, Andrews P, Kendall J, Leu J, Chunduri NK, Levy D, *et al* (2020) Single-Chromosomal Gains Can Function as Metastasis Suppressors and Promoters in Colon Cancer. *Developmental Cell* 52: 413-428.e6

Vasudevan A, Schukken KM, Sausville EL, Girish V, Adebambo OA & Sheltzer JM (2021) Aneuploidy as a promoter and suppressor of malignant growth. *Nat Rev Cancer* 21: 89–103

Weaver BA & Cleveland DW (2006) Does aneuploidy cause cancer? *Current Opinion in Cell Biology* 18: 658–667

Weaver BA & Cleveland DW (2008) The Aneuploidy Paradox in Cell Growth and Tumorigenesis. *Cancer Cell* 14: 431–433

Weaver BAA, Silk AD, Montagna C, Verdier-Pinard P & Cleveland DW (2007) Aneuploidy Acts Both Oncogenically and as a Tumor Suppressor. *Cancer Cell* 11: 25–36

Williams BR, Prabhu VR, Hunter KE, Glazier CM, Whittaker CA, Housman DE & Amon A (2008) Aneuploidy Affects Proliferation and Spontaneous Immortalization in Mammalian Cells. *Science* 322: 703–709

6 Zusammenfassung

Aneuploidie, ein Zustand, in dem Zellen eine abnormale Chromosomenzahl aufweisen, tritt oft in Krebs auf und beeinträchtigt für gewöhnlich das Zellwachstum. Paradoxerweise ist Aneuploide in vielen Tumoren vertreten, in denen sie Zellwachstum und Therapieresistenz begünstigt. Chromosomeninstabilität (CIN), welche aus einer erhöhten Fehlteilungsrate resultiert, kann adaptive Vorteile unter Stress bieten. CIN, ausgelöst durch bestimmte Medikamente, führt zu zellulärer Heterogenität, begleitet von bestimmten Chromosomenzuwächsen und -verlusten. In gesunden Zellen sorgt ein Überwachungsmechanismus namens Spindle Assembly Checkpoint (SAC, Spindel-Zusammenbau-Kontrollpunkt) für die korrekte Aufteilung der Chromosomen. Die Hemmung des SAC verkürzt die Mitose und resultiert in Fehlteilungen.

Die Adaptation von dipHAP1-Zellen an den CIN-induzierenden SAC-Inhibitor Reversine zeigte, dass der Verlust von Chromosom 6p oder 13q das Wachstum in Reversine durch Verlängerung der mitotischen Dauer förderte. SAC-Gene *p31^{comet}* und *CDC16* auf diesen Chromosomen wurden als Schlüsselgene für die Resistenz identifiziert (Adell & Klockner *et al*, 2023). Während dieser Arbeit habe ich die Überexpression der Gene *p31^{comet}* und *CDC16* in dipHAP1 Zelllinien, welche für diese Gene heterozygot waren, mittels CRISPRa getestet. Die Rolle dieser Gene in der Reversine-Resistenz wurde durch die messbare Verlängerung der Mitose im Anschluss an die Überexpression mit und ohne Reversine bestärkt. Durch Selektion von Reversine-adaptierten HAP1 und dipHAP1 Zelllinien mit spezifischen Chromosomenzuwachs testeten wir ihre Rolle in der Reversine-Resistenz. Durch CRISPR-Deletionen von den zusätzlichen Chromosomenarmen konnten wir zeigen, dass der Zuwachs von Chromosom-Arm 1q an der Reversine-Resistenz beteiligt ist, was nicht nur die Mitose-Dauer, sondern auch mitotische Fehler reduziert.

Keywords: Aneuploidie, Arzneimittelresistenz, Chromosomenzuwachs und -verlust

7 Supplement

7.1 Supplemental experiments

7.1.1 Role of chromosome 11 acquisition during reversine adaptation unclear

Additionally to the HAP1 cell lines 4F, 4C and 2C, the adapted cell line 1D was checked for chromosome gains, as we were interested in it for gains of chromosome 8 (Figure 8). The qPCR (Supplemental Figure 1) showed some of the 1D derived cell line had gains of chromosome 8, but a more prevalent karyotype alteration was gain of chr 11, which some cell lines gained multiple of. For some of them, it was not clear whether they gained chr 8 at all as they just showed a slight increase, not the expected 2-fold amplification. The sequencing results for 1D 8, 17 and 24 can be found in Supplemental Figure 8. In the CFA, under standard conditions, most 1D cell lines grew half as well as WT, while upon reversine addition, rescue was extremely divers. Cell lines that presumably gained multiple copies of chr. 11 often had a better rescue (1D 2, 1D 5 and 1D 9) than cell lines that did not or only had slight increases in chr. 11 levels. However, 1D 11 with approximately the same chr. 11 levels grew much worse than comparable cell lines 1D 2 or 1D 5. 1D 17 and 1D 24, negative for both 8 and 11 gain, did not have any rescue at all, while 1D 8, having a gain in both 8 and 11, rescued only minimally better than WT. While

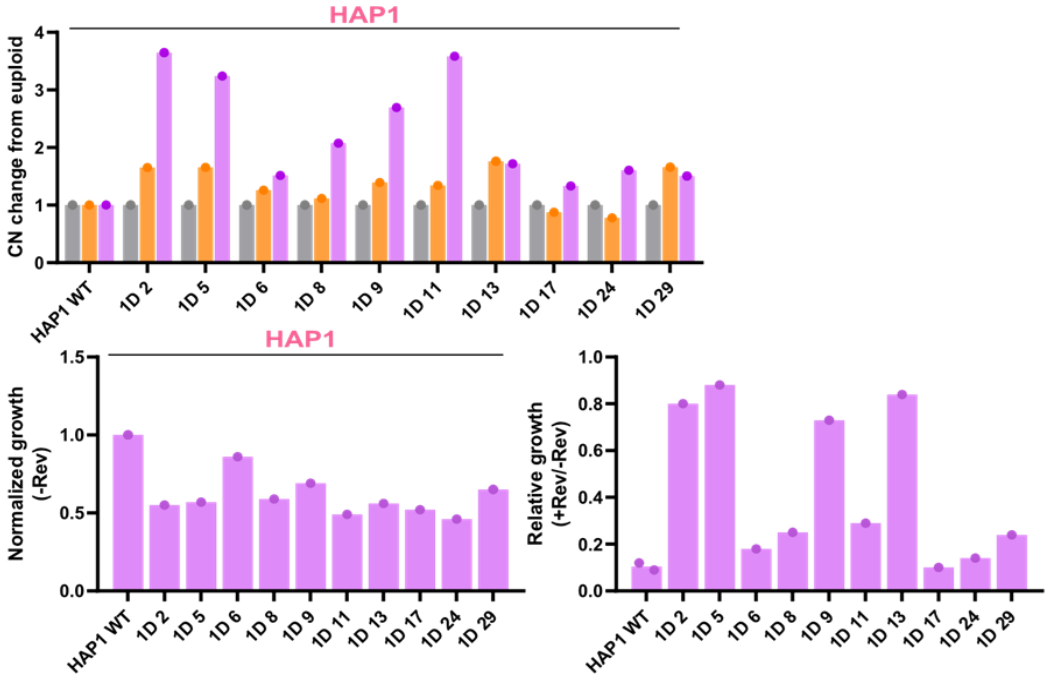

Supplemental Figure 1: qPCR and colony formation assay results for HAP1 1D cell lines.

in the qPCR it seemed that 1D 8 only gained 11, it also had a gain in chr 8, so qPCR results for this chromosome do not seem very reliable in this case. Chromosome 11 gain might contribute to reversine resistance, however, without confirmation via sequencing, this is mostly speculation. As the combined gain of one copy of chromosome 8 and 11 showed just a slight increase in resistance compared to gaining multiple chr. 11 copies, there could be a negative correlation between acquisition of these gains.

7.1.2 Scratch assay and influence of different chromosomes for #4 cell lines

To try another method of researching differences between cell lines, we conducted a scratch assay for the dipHAP1 #4 cell lines (Supplemental Figure 2). DipHAP1 #4 1, #4 3 and 17 had roughly the same closing rate as WT, while cells of dipHAP1 #4 7 and #4 14 migrated 2x and 1.5x as fast as WT, respectively. Comparing their karyotype (Table 2), loss of chr. 14 could influence the closing rate. In #4 17, loss of chr. 14 does not seem to have the same effect. However, loss of chromosome 7 possibly negates this migration advantage.

All in all, this first scratch assay data could indicate loss of chr. 14 increases migration potential of dipHAP1 cells.

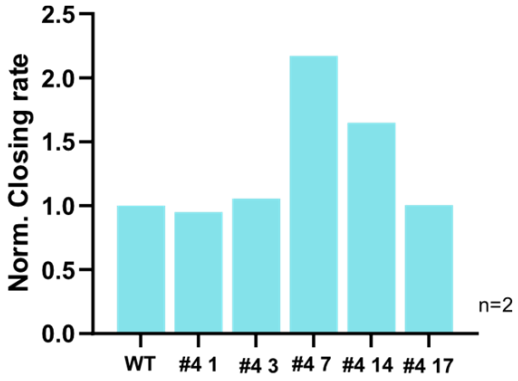

Supplemental Figure 2: Scratch assay results for #4 cell lines depicted as normalized closing rate. Bars depict +/- SD.

7.2 Supplemental Figures

7.2.1 Karyotype data for parental CRISPRa cell lines

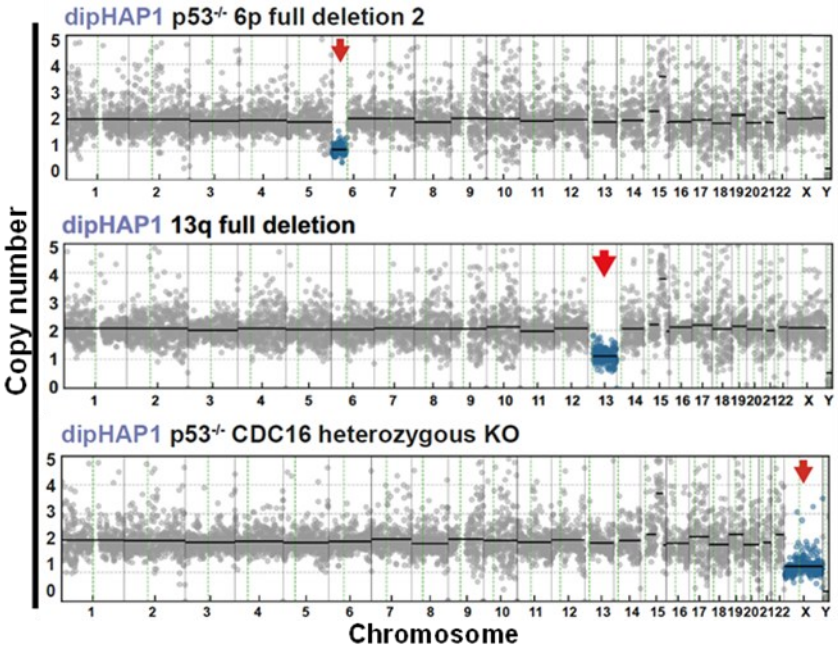

Supplemental Figure 3: Copy number profiles of dipHAP1 cells engineered for either 13q or 6p loss or CDC16+/- knockdown from Adell & Klockner et al., 2023. Blue dots marked with an arrow represent chromosome losses.

7.2.2 qPCR data to identify cell lines with specific chromosome gains

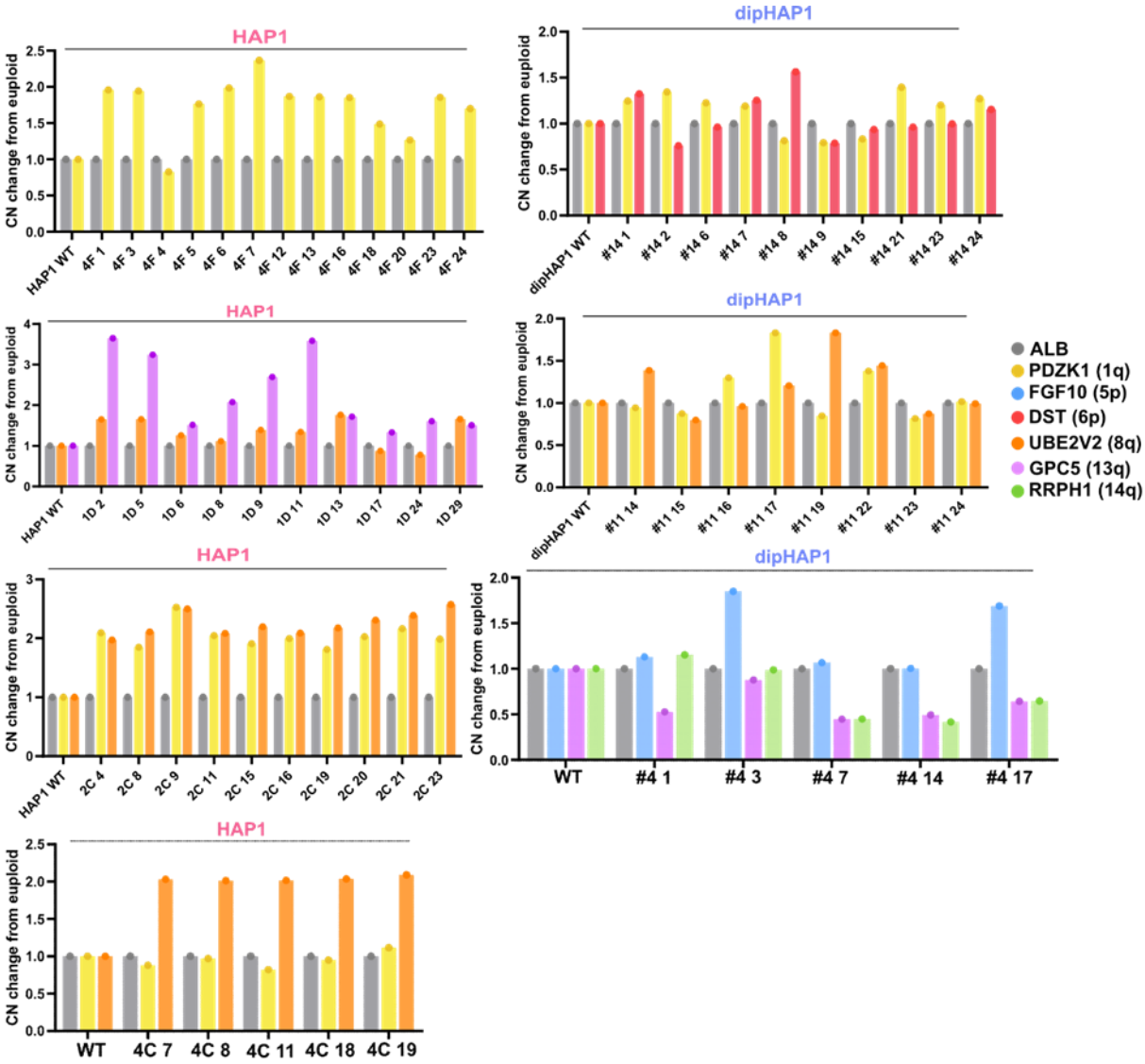

Supplemental Figure 4: Supplemental qPCR results for HAP1 and dipHAP1 cell lines. CN change from euploid is normalized to either HAP1 or dipHAP1 WT.

7.2.3 CFA data for additional chromosome gain cell lines

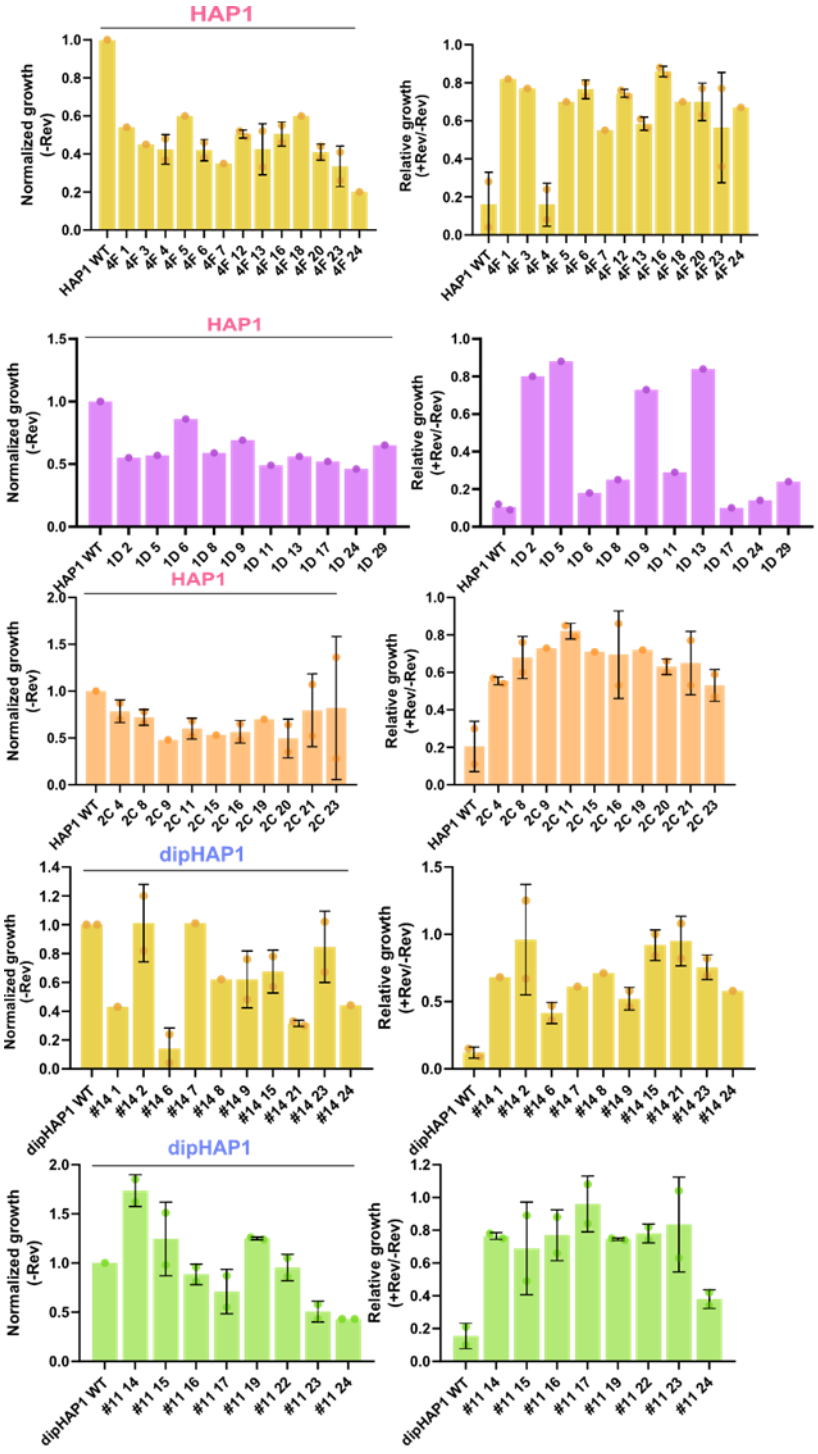

Supplemental Figure 5: Normalized and relative growth of depicted HAP1 or dipHAP1 cell lines measured via colony formation assay; n= number of dots per bar graph, n=3 for all WT.

7.2.4 qPCR, CFA and scratch assay data for additional CRISPR-del cell lines

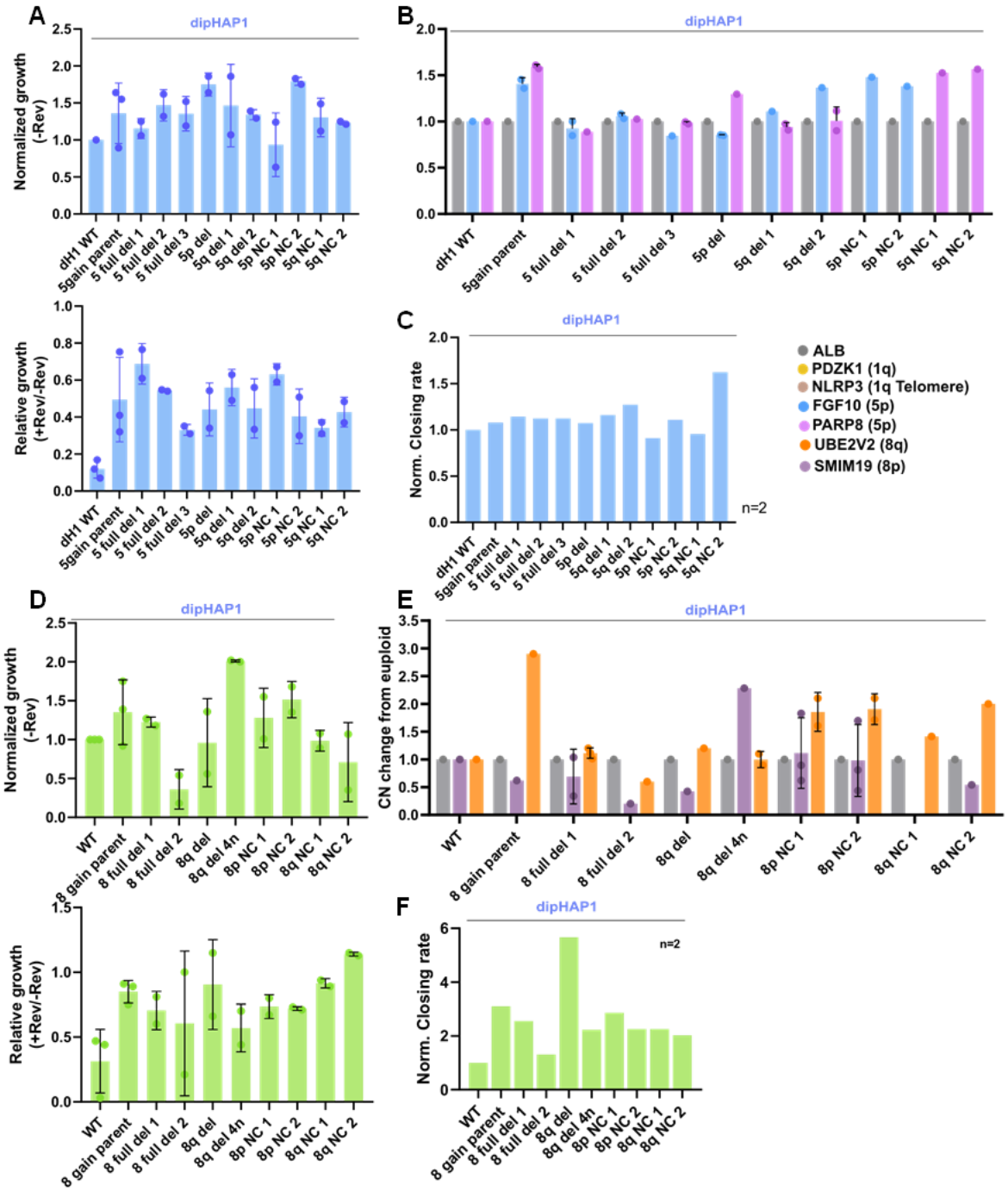

Supplemental Figure 6: Additional CFA (A, D) qPCR (B, E) and scratch assay (C, F) data for dipHAP1 5 gain/del and 8 gain/del cell lines. n=number of dots per bar graph, n=3 for WT.

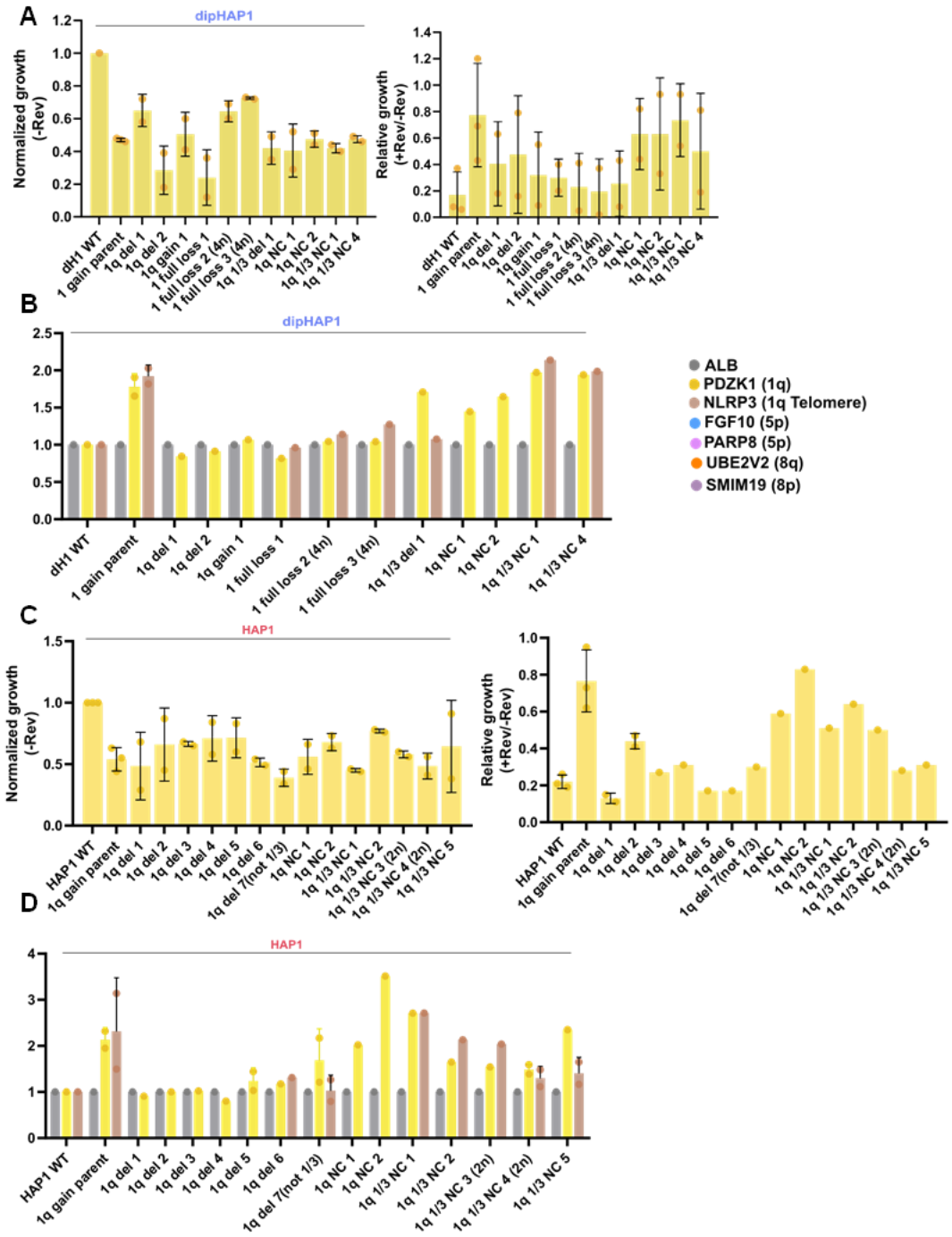

Supplemental Figure 7: Additional CFA (A, C) and qPCR (B, D) data for HAP1 and dipHAP1 1(q) gain/del cell lines. n=number of dots per bar graph, n=3 for WT.

7.2.5 Karyotypes of chromosome gain cell lines

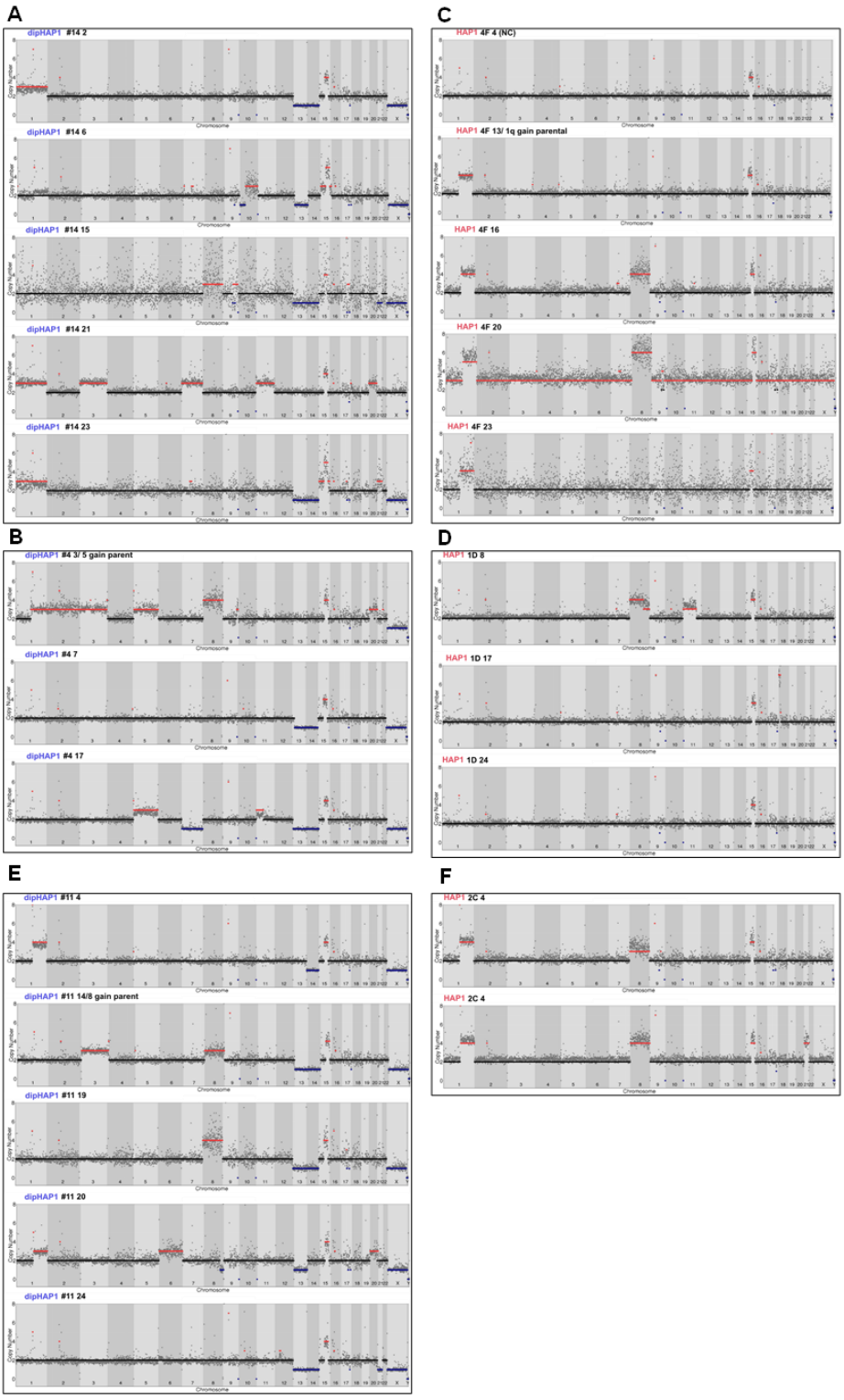

Supplemental Figure 8: Copy number profiles of chromosome gain cell lines. Blue dots represent losses, while red dots represent gains.

7.2.6 *Karyotypes of CRISPRdel cell lines*

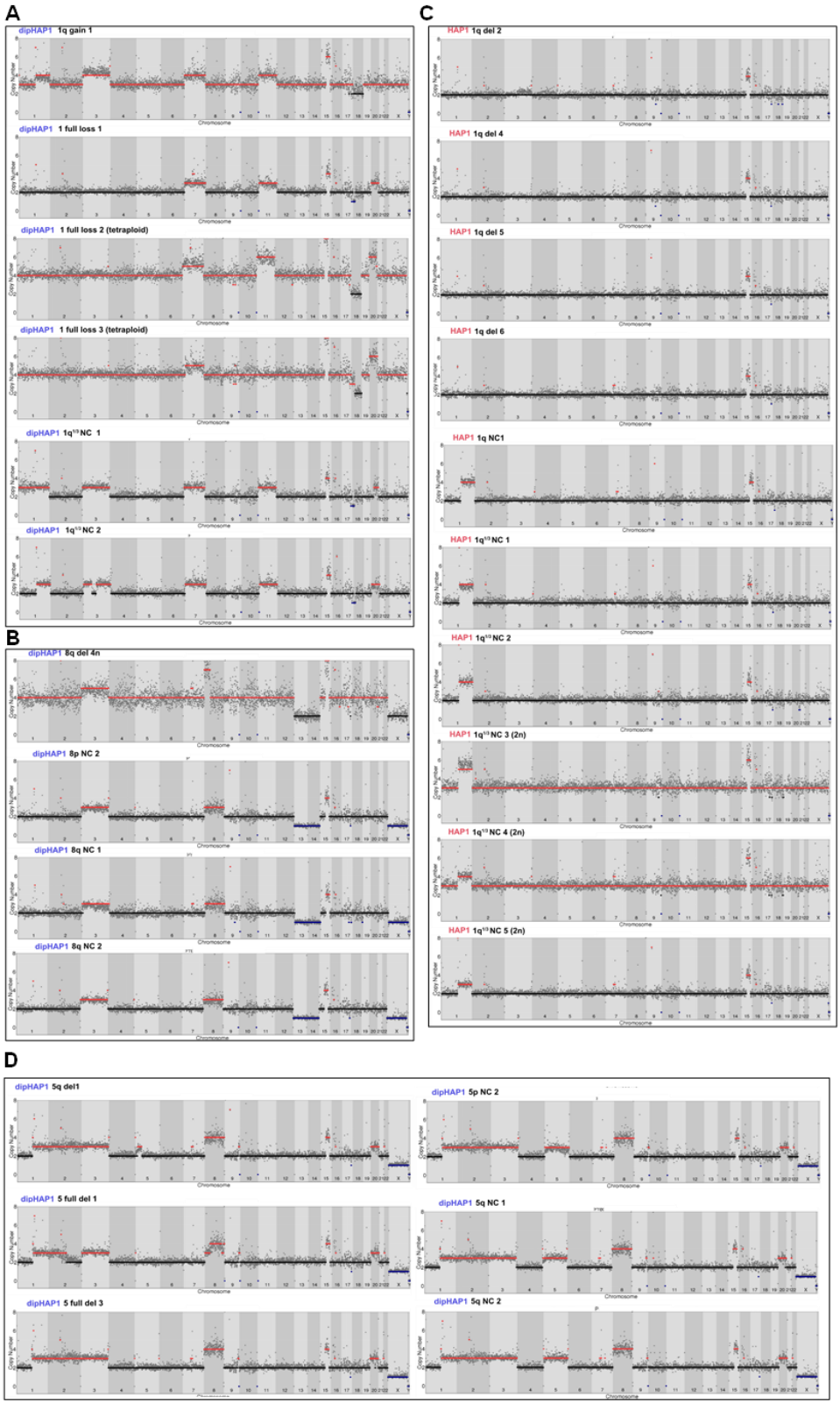

Supplemental Figure 9: Copy number profiles of chromosome gain CRIPSR deletion cell lines. Blue dots represent losses, while red dots represent gains.

7.2.7 Flow cytometry ploidy data of HAP1 cells

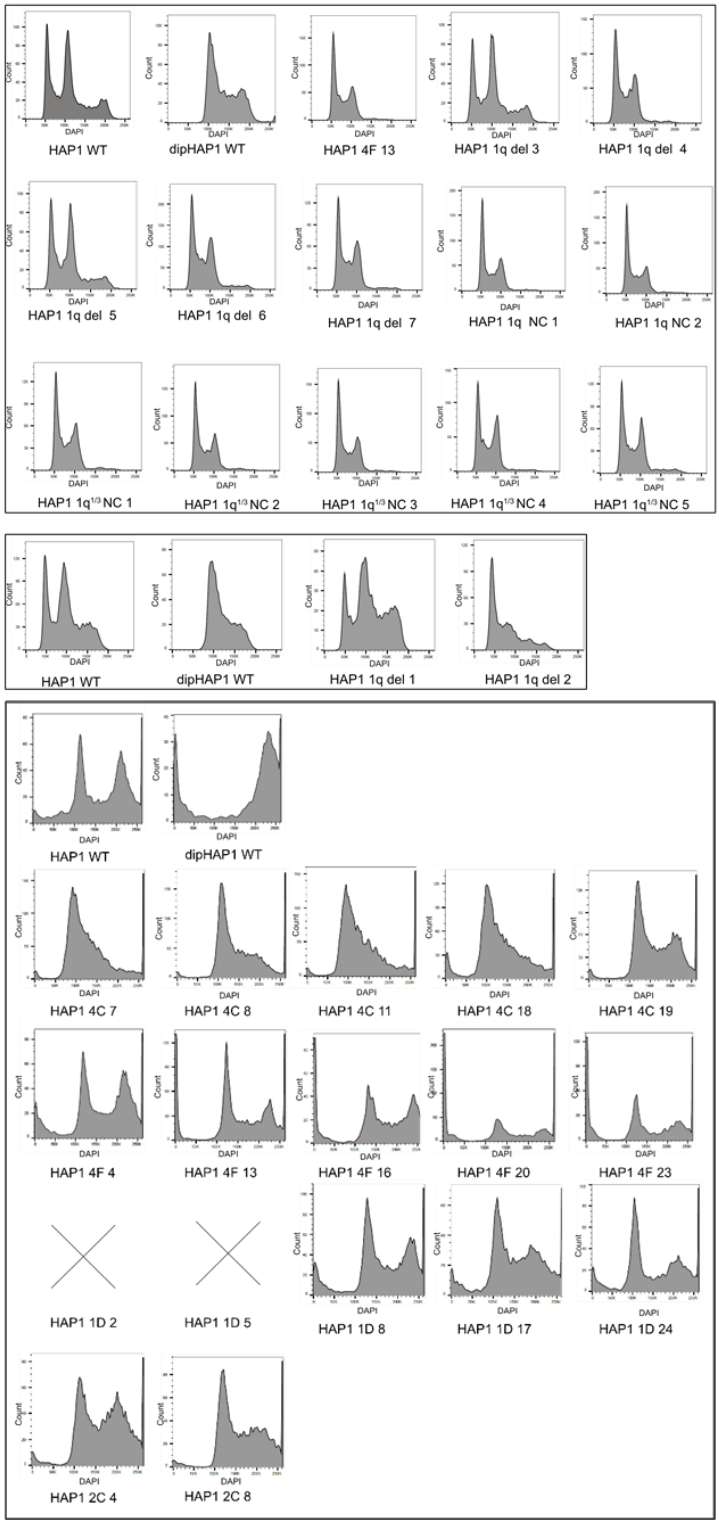

Supplemental Figure 10: Ploidy assessment in HAP1 cell lines. dipHAP1 WT and HAP1 WT for comparisons to cell lines from the same experiment are depeicted in the same box as samples.

7.3 List of Figures

7.4 List of tables

7.5 List of supplemental figures

7.6 Supplemental Tables

7.6.1 Name conversion chart for cell lines

Table 3: Conversion chart for names of cell lines.

Name during experiments:	Name in Thesis:	Used CRISPR guide:	Name during experiments:	Name in Thesis:	Used CRISP guide:
4F 13	4F 13/ 1q gain parent		**#14 21**	#14 21/ 1 gain parent	
4F 13 1q2 (del) (old)	1q del 1	1q (old)	**#14 1q 8 (del)**	1q del 1	1q (new)
4F 13 1q3 (del) (old)	1q del 2	1q (old)	**#14 1q 12 (del)**	1q del 2	1q (new)
4F 13 1q6 (del)	1q del 3	1q (new)	**#14 1q 13 (del)**	1q gain 1	1q (new)
4F 13 1q7 (del)	1q del 4	1q (new)	**#14 1q 1/3 12 (full del)**	1 full loss 1	1q 1/3 (new)
4F 13 1q10 (del)	1q del 5	1q (new)	**#14 1q 1/3 19 (full del)**	1 full loss 2 (4n)	1q 1/3 (new)
4F13 1q1/3 25 (full del)	1q del 6	1q 1/3 (new)	**#14 1q 1/3 23 (full del)**	1 full loss 3 (4n)	1q 1/3 (new)
4F13 1q1/3 3 (del)	1q del 7(not 1/3)	1q 1/3 (new)	**#14 1q 1/3 15 (del)**	1q 1/3 del 1	1q 1/3 (new)
4F 13 1q11 (NC)	1q NC 1	1q (new)	**#14 1q 5 (NC)**	1q NC 1	1q (new)
4F13 1q14 (NC)	1q NC 2	1q (new)	**#14 1q 6 (NC)**	1q NC 2	1q (new)
4F13 1q1/3 9 (NC)	1q 1/3 NC 1	1q 1/3 (new)	**#14 1q 1/3 2 (NC)**	1q 1/3 NC 1	1q 1/3 (new)
4F 1q1/3 27 (NC)	1q 1/3 NC 2	1q 1/3 (new)	**#14 1q 1/3 8 (NC)**	1q 1/3 NC 4	1q 1/3 (new)
4F 1q1/3 28 (NC)	1q 1/3 NC 3 (2n)	1q 1/3 (new)			
4F 1q1/3 33 (NC)	1q 1/3 NC 4 (2n)	1q 1/3 (new)	**#4 3**	#4 3/ 5gain parent	
4F 1q1/3 36 (NC)	1q 1/3 NC 5	1q 1/3 (new)	**5p8 (full del)**	5 full del 1	5p (new)
			5p17 (full del)	5 full del 2	5p (new)
#11 14	#11 14/ 8 gain parent		**5q19 (full del)**	5 full del 3	5q (new)
#11 14 8(q) 10 (full del)	8 full del 1	8q (old)	**5p10 (del)**	5p del	5p (new)
#11 14 8(q) 12 (full del)	8 full del 2	8q (old)	**5q13 (del)**	5q del 1	5q (new)
#11 14 8p 6 (del)	8q del	8p (old)	**5q24 (del)**	5q del 2	5q (new)
#11 14 8q 9 (del)	8q del 4n	8q (old)	**5p1 (NC)**	5p NC 1	5p (new)
#11 14 8p 1 (NC)	8p NC 1	8p (old)	**5p2 (NC)**	5p NC 2	5p (new)
#11 14 8p 3 (NC)	8p NC 2	8p (old)	**5q1 (NC)**	5q NC 1	5q (new)
#11 14 8q 4 (NC)	8q NC 1	8q (old)	**5q2 (NC)**	5q NC 2	5q (new)
#11 14 8q 14 (NC)	8q NC 2	8q (old)			

7.6.2 qPCR primers to identify chromosome gains or losses

Table 4: qPCR primers to identify chromosome losses or gains.

Name	Sequence	
ALB	fwd	TGTTGCATGAGAAAACGCCA
	rev	GTCGCCTGTTCAACCAAGGAT
PDZK1 **(1q Centromere)**	fwd	AGGATCTCTTCAGCCCCCACA
	rev	ACAGTTCTTGGTTCCTCATAGGG
NLRP3 **(1q Telomere)**	fwd	GGGCAGAACTTGTCCTGGTT
	rev	TTGCACACGTAGAGCCCAAA
FGF10 **(5p)**	fwd	GGAAGAGCTGGGGATGCTAC
	rev	CTTTGAGGGCTAGGTTCCCG
PARP8 **(5q)**	fwd	ACCCTGAGTAAAGGGTCGCT
	rev	CATGCTTTCCCAACGACTGC
DST **(6p)**	fwd	CTACCAGCACTCGAACCAGTC
	rev	GCCGAAGCTAATGCAAGAGTTG
SMIM19 **(8p)**	fwd	TCATGATTGAGGACTGGGCG
	rev	GTCACTCTTCTGCGCTTCCA
UBE2V2 **(8q)**	fwd	AGTTCCTCGTAATTTTCGCTTGT
	rev	CCCCAGCTAACTGTACCGT
ART5 **(11p)**	fwd	GCCTCCTTGGGTTACCTGTG
	rev	TGAGCTCTGAGACGCCTGAG
GPC5 **(13q)**	fwd	GGTGTGACTGACAGTTCCCTG
	rev	TGCAGATAGTCTGTGGTGTTGAT
RPPH1 **(14q)**	fwd	CCACGAGCTGAGTGCGT
	rev	CTGCCCAGTCTGACCTCG
TPX2 **(20q)**	fwd	ACTTCCGCACAGATGAGCG
	rev	GGATGCTTTCGTAGTTCAGATGT

7.6.3 sgRNAs used for CRISPR activation

Table 5: sgRNAs used for CRISPRa.

Name	Sequence	
sgRNA *p31^{comet}* 3x and for *p31^{comet}* Gibson plasmid		
1	fwd	caccGCGTCGCCGCAGTGTGGGGG
	rev	aaacCCCCCACACTGCGGCGACGC
2	fwd	caccGCGCGGGCCCCGTGCTCAAG
	rev	aaacCTTGAGCACGGGGCCCGCGC
3	fwd	caccGTAACCTAGCGTAGTCACAGT
	rev	aaacACTGTGACTACGCTAGGTTAC
sgRNA *CDC16*		
C1	fwd	caccGTGGGCTTCTGGTTGCCTTG
	rev	aaacCAAGGCAACCAGAAGCCCAC
sgRNA *TTN*	fwd	caccCCTTGGTGAAGTCTCCTTTG
	rev	aaacCAAAGGAGACTTCACCAAGG

7.6.4 Fragments for generation of p31 Gibson plasmid

Table 6: Primers for fragment creation for Gibson.

Fragment name	Primer sequence		Template
1	fwd	GTAACAAGCGGGTGTTCTCT	p31^{comet} sgRNA 1
	rev	CGGGTTTATTACAGGGACAG	
2	fwd	CTGTCCCTGTAATAAACCCGCCGGTAGAATTAGATCGCTA	p31^{comet} sgRNA 2
	rev	TTGGTCCCTACGATTAAGCAGCAGAGATCCAGTTTGGT	
3	fwd	GGCAGCACTGCATAATTCT	p31^{comet} sgRNA 3
	rev	CTTAATCGTAGGGACCAAGGTAGAATTAGATCGCTAGC	
4	fwd	AGAATTATGCAGTGCTGCC	p31^{comet} sgRNA 1
	rev	AGAGAACACCCGCTTGTTAC	

7.6.5 sgRNAs used for CRISPR deletion of chromosome gains

Table 7: sgRNAs used for CRISPR deletion of chromosome gains.

Name	Sequence	
Chromosome arm 1q		
sgRNA 1q (old)	fwd	caccGTAAGTCCCGCTCCGATTGCG
	rev	aaacCGCAATCGGAGCGGGACTTAC
sgRNA 1q (new)	fwd	caccGATCATCGAAATGGACTCAAA
	rev	aaacTTTGAGTCCATTTCGATGATC
sgRNA 1q 1/3	fwd	caccGACGTGTTGTCGGTTATCTAC
	rev	aaacGTAGATAACCGACAACACGTC
Chromosome arm 5		
sgRNA 5p	fwd	caccGACGGACTTAACTTGGTGTTA
	rev	aaacTAACACCAAGTTAAGTCCGTC
sgRNA 5q	fwd	caccGACACTTTGCCTTAGGGGTAT
	rev	aaacATACCCCTAAGGCAAAGTGTC
Chromosome arm 8		
sgRNA 8p	fwd	caccGTGGGCCGTTCGATACCTCTA
	rev	aaacTAGAGGTATCGAACGGCCCAC
sgRNA 8q	fwd	caccGCTTGCGTAGGACGGTCGTCG
	rev	aaacCGACGACCGTCCTACGCAAGC

7.6.6 RTqPCR primers for CRISPRa

Table 8: RTqPCR primers to assess fold induction in CRISPRa experiments.

Name	Sequence	
GAPDH	fwd	TTGACCTCAACTACATGGTTTAC
	rev	AGGAGGCATTGCTGATGATC
CDC16	fwd	TCCTGTGTCTTGGTTTGCAG
	rev	CAGAGCTTGGCTGAAGAACC
P31	fwd	GAGAAGTCCGAAGAAACTCACG
	rev	CCGAAGCGTTGAGAGGTTCC
TTN	fwd	TGTTGCCACTGGTGCTAAAG
	rev	ACAGCAGTCTTCTCCGCTTC

7.6.7 List of cell lines used

Table 9: Cell lines used.

Cell line	Tissue
diploid HAP1 (dipHAP1) TP53 KO	Chronic myeloid leukemia (CML)
haploid HAP1 TP 53 KO	Chronic myeloid leukemia (CML)
HEK293 HiEx	Human embryonic kidney

7.6.8 List of plasmids used

Table 10: List of plasmids used and description.

Plasmid	Usage
dCas9-VPR-mCherry	dCas9-VPR-mCherry fusion protein expressing plasmid for generating lentivirus to be used in CRISPRa
po88$_2$	Lentiviral packaging plasmid
pMD2.G VSV-plasmid	VSV-envelope expressing plasmid for lentivirus generation
sgRNA-GFP-Neo^R	Plasmid expressing GFP with neomycin resistance for sgRNA delivery without Cas9
sgRNA-GFP-Neo^R GIbson	Same plasmid as sgRNA-GFP-NeoR with 3 p31 guides cloned into sgRNA site via Gibson
pSpCas9(BB)-2A-GFP (PX458)	Plasmid expressing Cas9 with EGFP and backbone for sgRNAs for CRISPR deletions

7.6.9 GAPDH value variability

Table 11: GAPDH RTqPCR value variability. GAPDH Ct value average for 3 samples.

Cell line + sgRNA	RT-qPCR	GAPDH
dCas9-VPR-WT + empty 1	1	15,25
dCas9-VPR-WT + CDC16-C1 1	1	16,95
dCas9-VPR-WT + empty 2	2	19,05
dCas9-VPR-WT + CDC16-C1 2	2	18,14
dCas9-VPR-WT + empty 3	3	17,19
dCas9-VPR-WT + CDC16-C1 3	3	27,46